Electrochemistry for Materials Technology

Chapter Z: Electrochemical Impedance Spectroscopy (EIS)

Part I: Fundamentals of Dielectric Spectroscopy

1 – Electrochemical interfacial processes

2 – Principle of impedance spectroscopy

3 – Ideal Circuit elements

4 – Case study 1: the RC element

5 – Representing EIS data: Bode and Nyquist plots

6 – Treatment of a ZARC element

7 – Faradaic reaction: the Randles circuit

8 – Non ideal elements

Part II: Practical aspects and data treatment

1 – Impedance measurements

2 – Data treatment

3 – Non-linear systems: Total Harmonic Distorsion

I) Fundamentals of EIS

1) Electrochemical interfacial processes

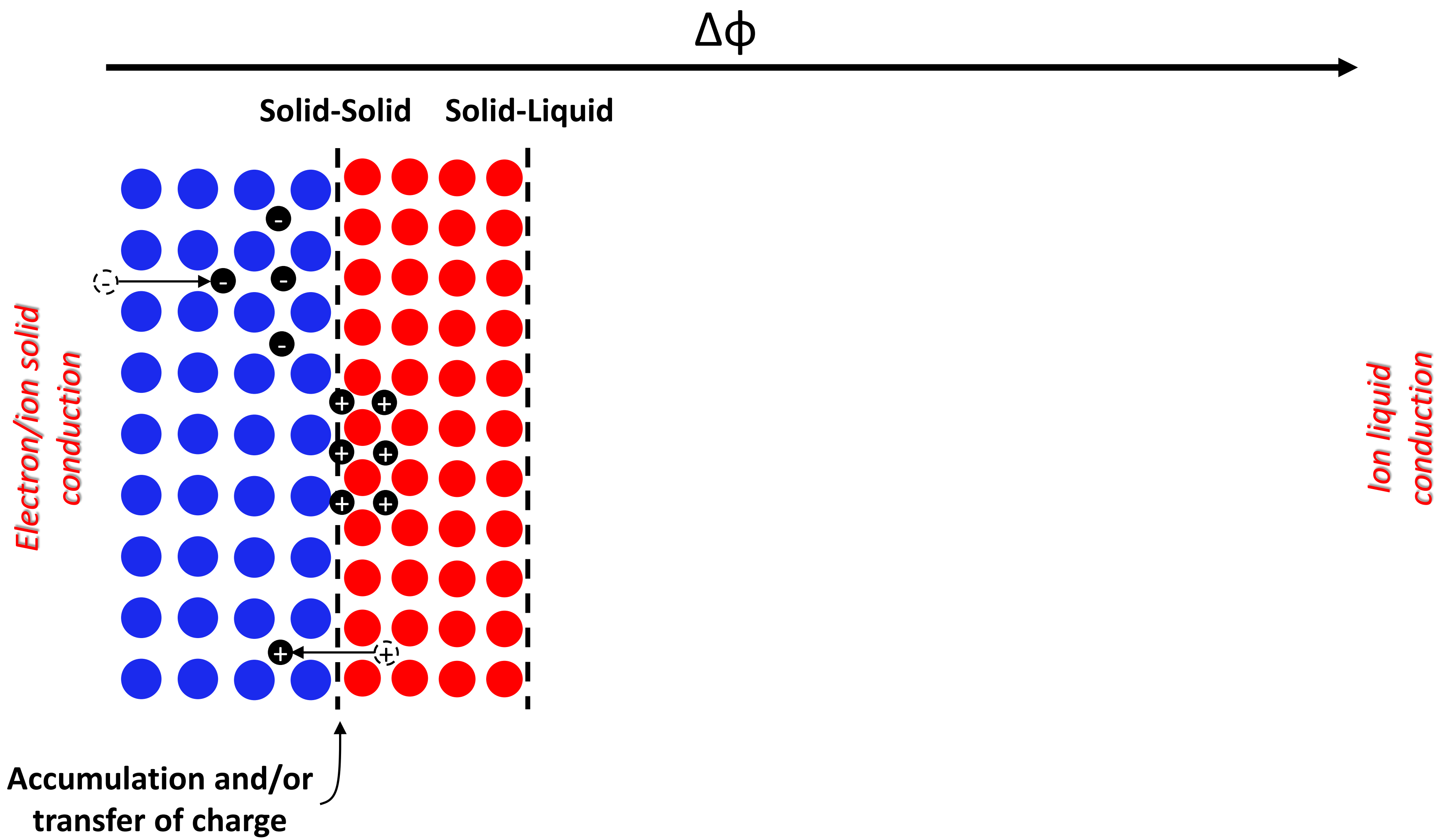

I) Fundamentals of EIS

1) Electrochemical interfacial processes

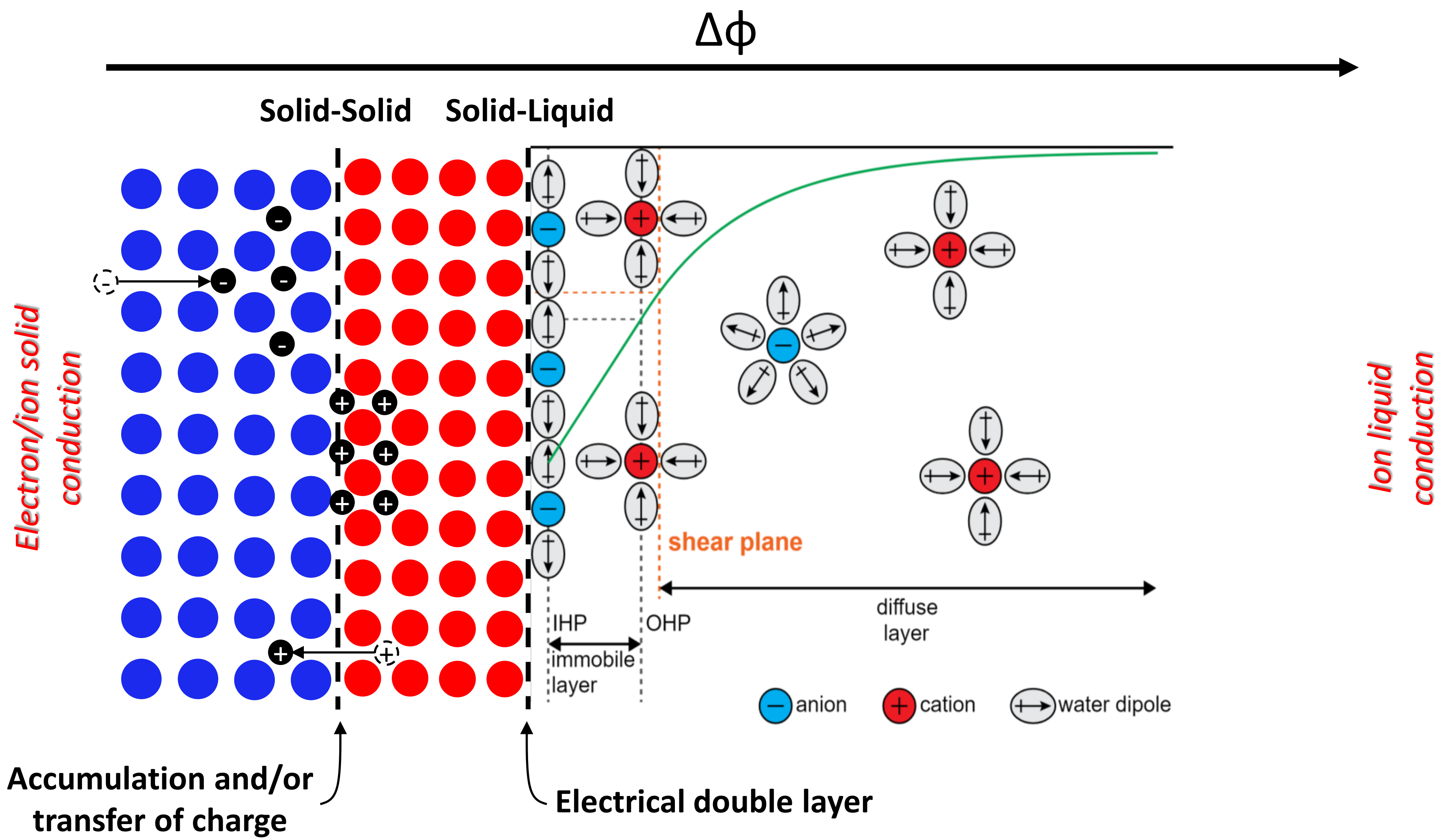

I) Fundamentals of EIS

1) Electrochemical interfacial processes

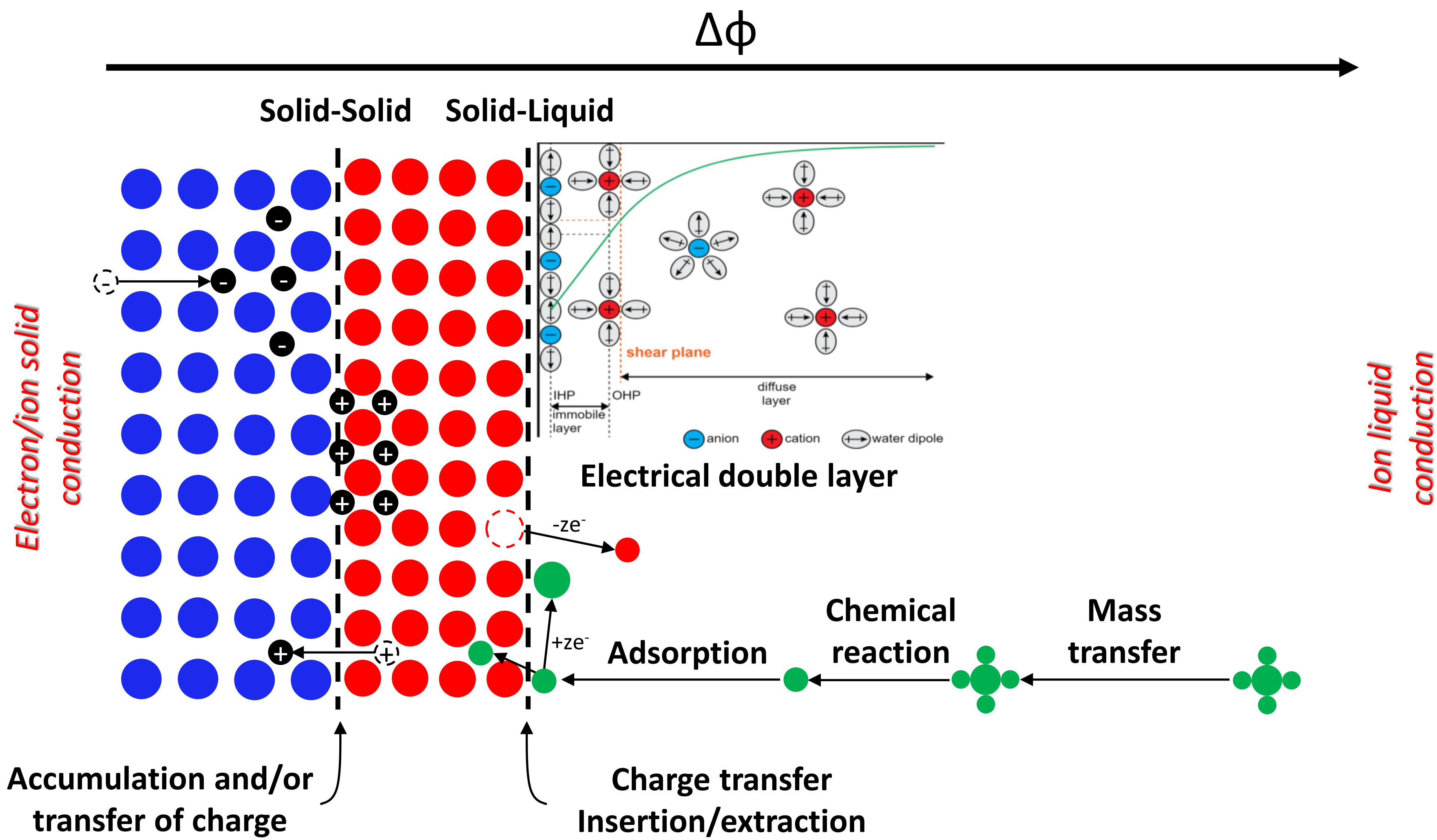

Process rates **≈1 MHz — 100 kHz — 1 kHz — 10 Hz — 100 mHz**

I) Fundamentals of EIS

1) Electrochemical interfacial processes

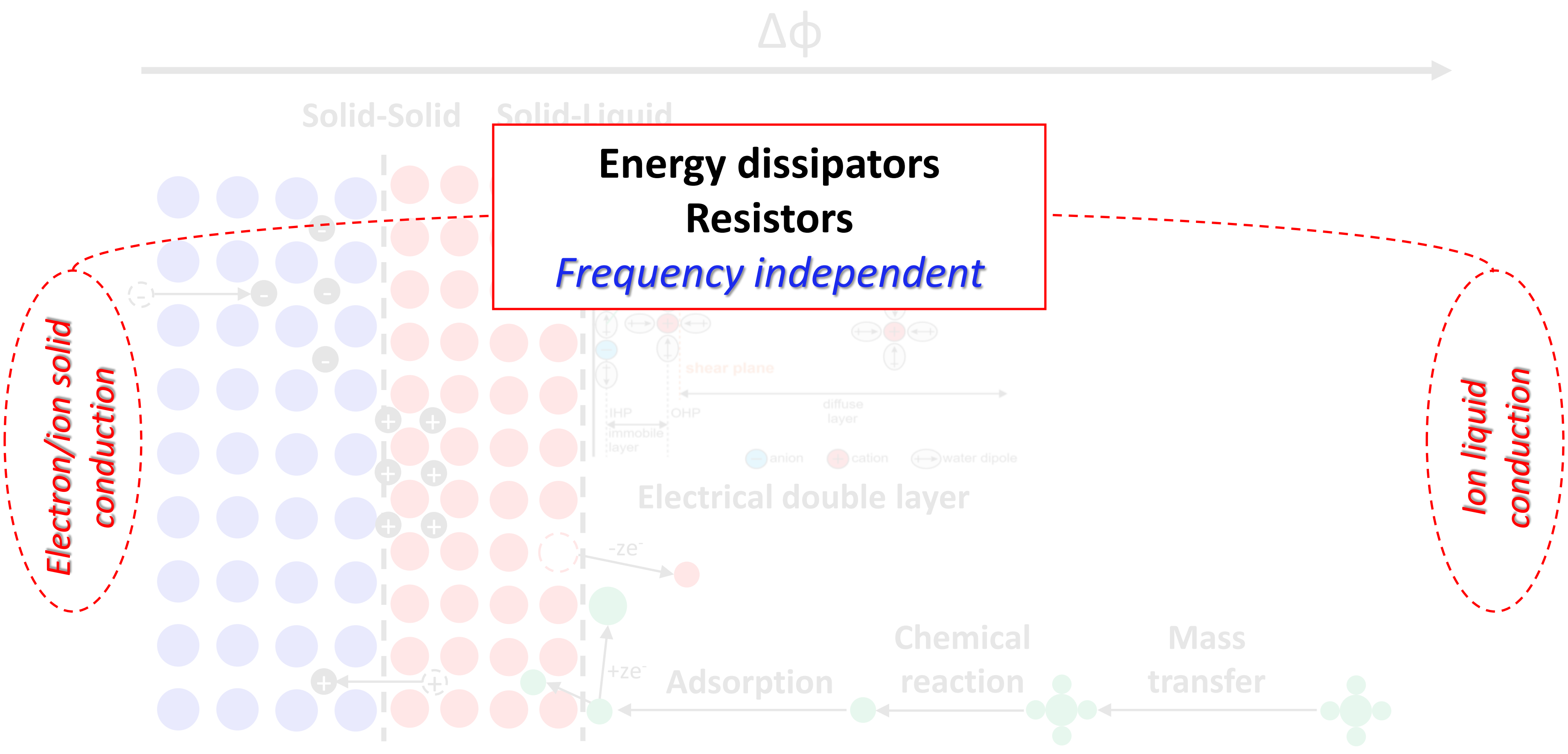

I) Fundamentals of EIS

1) Electrochemical interfacial processes

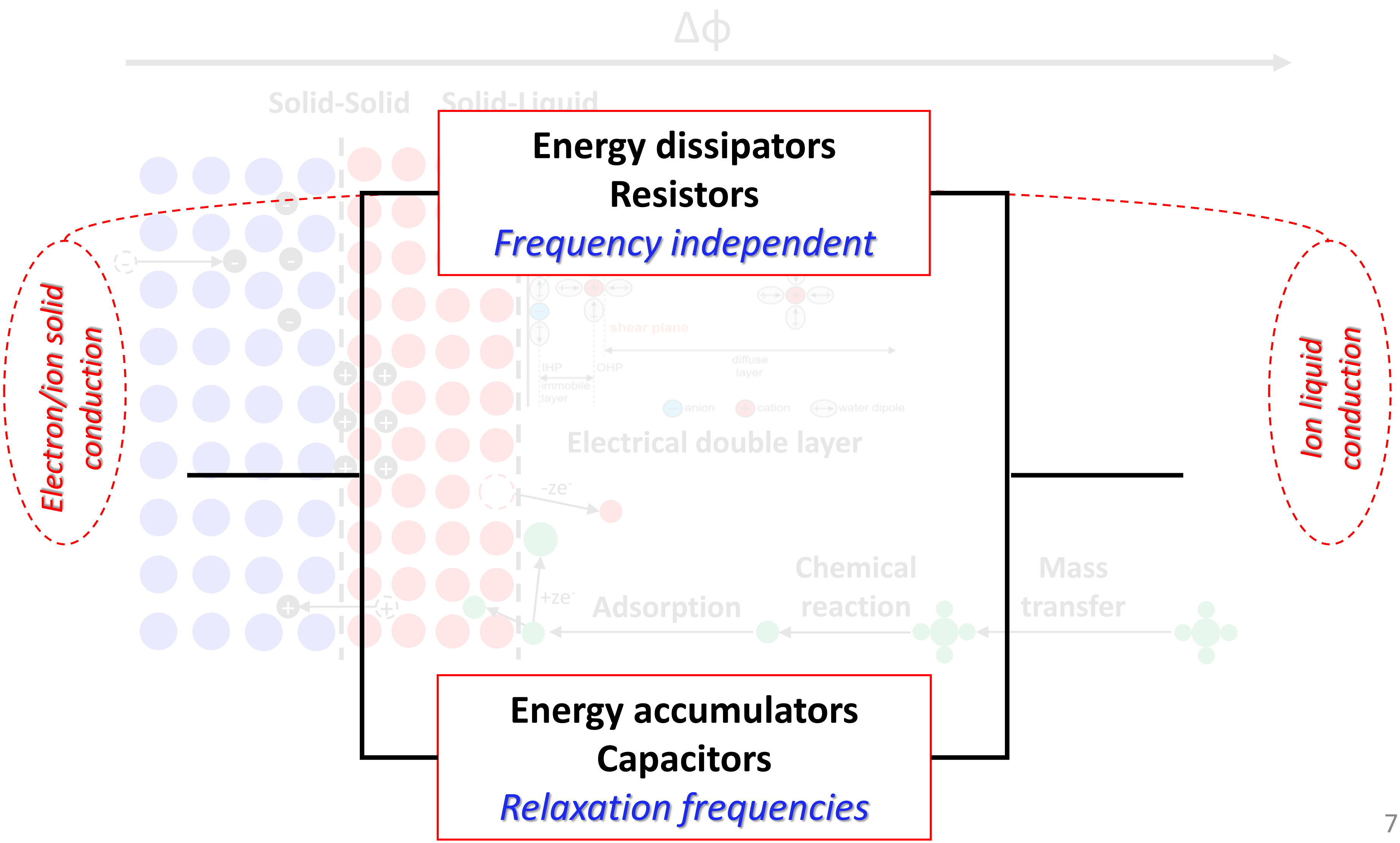

I) Fundamentals of EIS

2) Principle of impedance spectroscopy

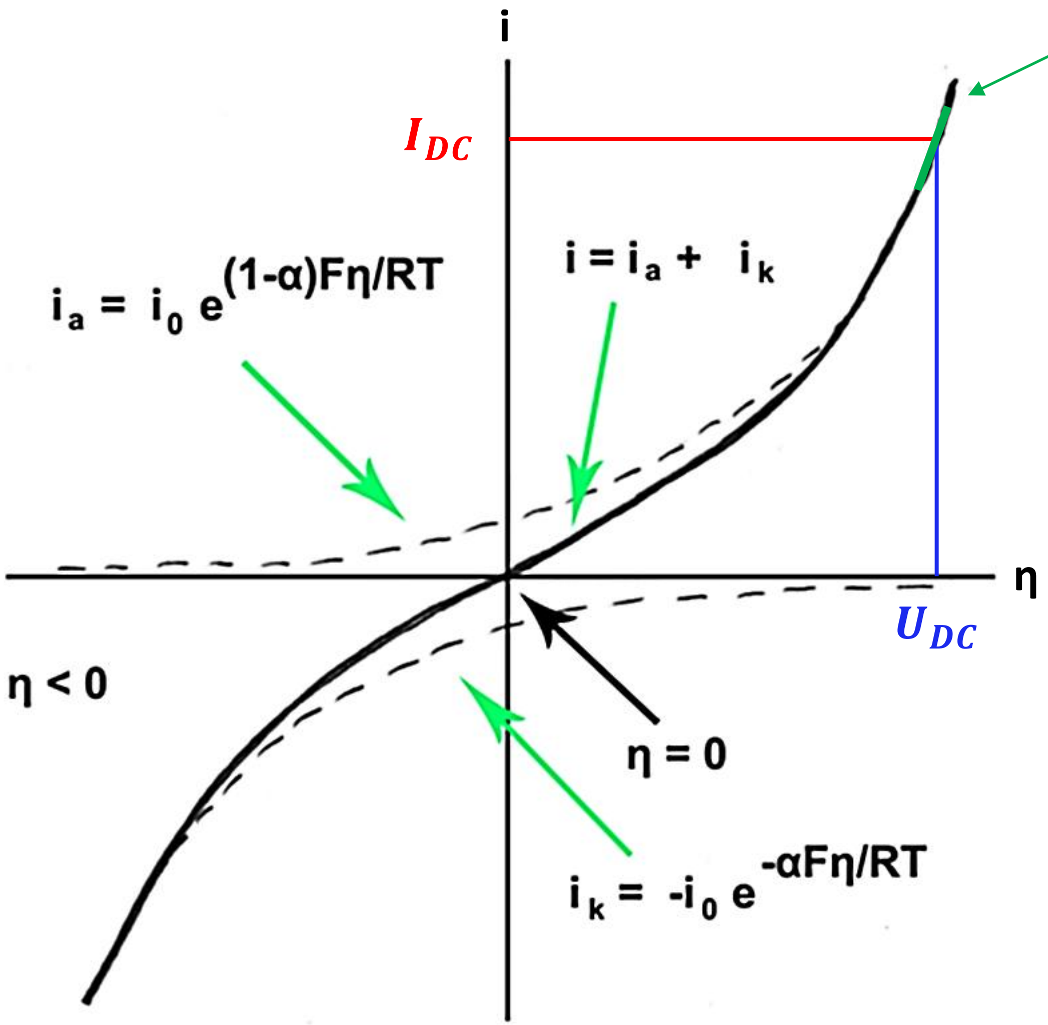

Local ASR (Area Specific Resistance)

$$ASR = \lim_{\Delta U \to 0} \left(\frac{\Delta U}{\Delta i} \right)$$

Only measures dissipators !

I) Fundamentals of EIS

2) Principle of impedance spectroscopy

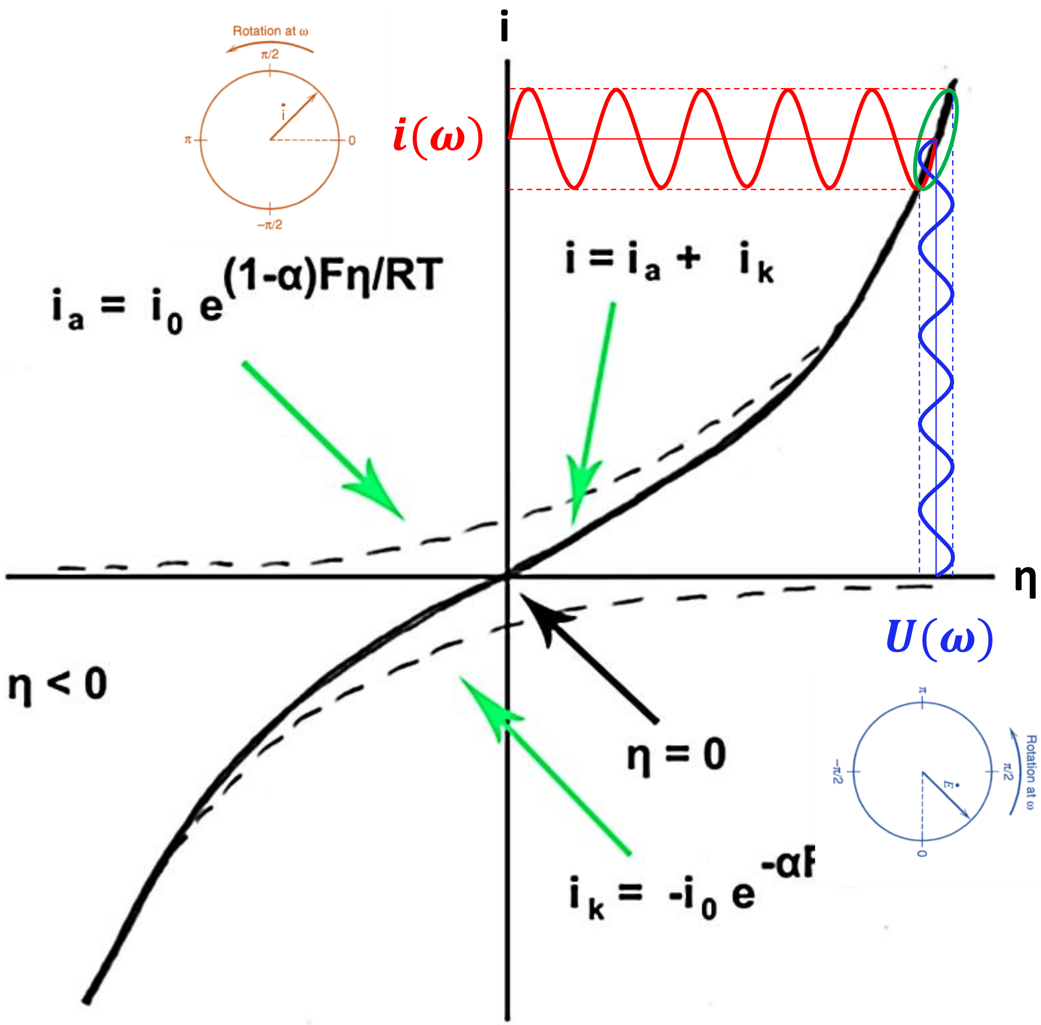

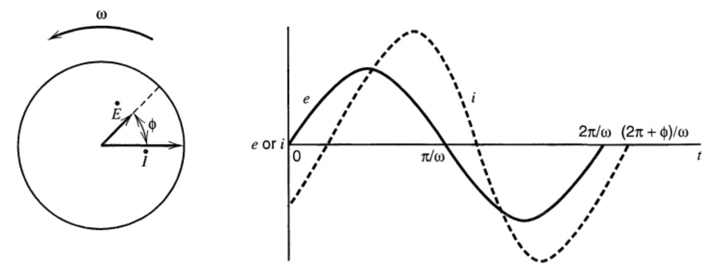

$i(\omega) = i_{DC} + \Delta i \sin(\omega t)$

$U(\omega) = U_{DC} + \Delta U \sin(\omega t + \varphi(\omega))$

Small excitation amplitude

↪ *Harmonic free linear response*

Measure of the complex impedance:

$$\tilde{Z}(\omega) = \frac{U(\omega)}{i(\omega)}$$

$\tilde{Z}(\omega)$ from 1 mHz to 1 MHz

I) Fundamentals of EIS

2) Principle of impedance spectroscopy

$$\tilde{Z}(\omega) = \frac{U_0 \sin(\omega t + \varphi)}{i_0 \sin(wt)}$$

$$\tilde{Z}(\omega) = \frac{U_0}{i_0} \cdot \frac{e^{j(\omega t+\varphi)} - e^{-j(\omega t+\varphi)}}{e^{j\omega t} - e^{-j\omega t}} = \frac{U_0}{i_0} \cdot e^{j\varphi}$$

$$\tilde{Z}(\omega) = \frac{U_0}{i_0} \cdot (\cos\varphi + j\sin\varphi)$$

$$\tilde{Z}(\omega) = Z_{Re} + jZ_{Im}$$

Vector representation:

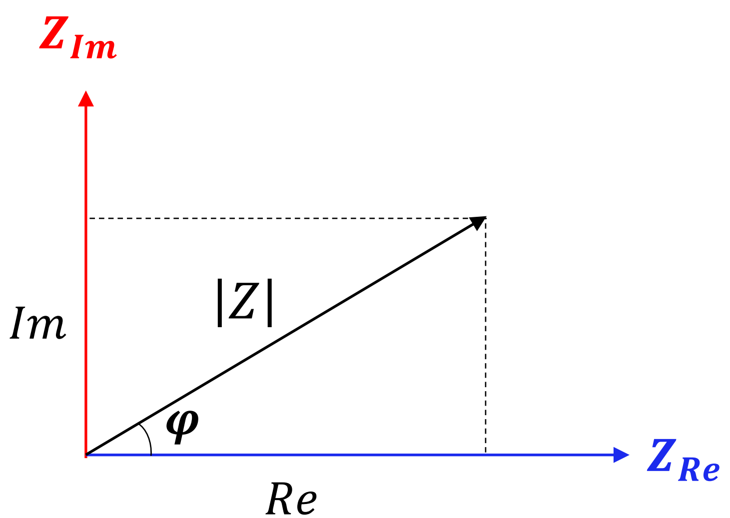

I) Fundamentals of EIS

3) Ideal circuit elements

Element	$U(\omega)$, $i(\omega)$	Phase shift φ	$\tilde{Z}(\omega)$
Resistor 	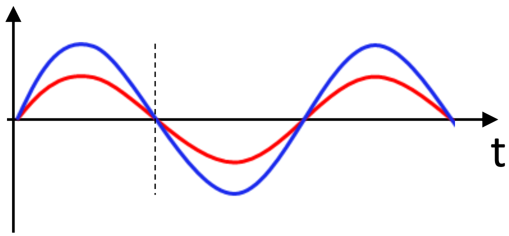	$\varphi = 0$ Current and volage in phase	$\tilde{Z}(\omega) = R$
Capacitor 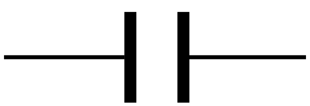	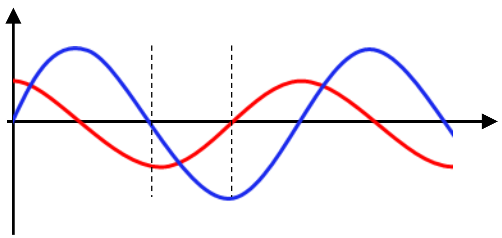	$\varphi = -\frac{\pi}{2}$ Current leads the voltage	$\tilde{Z}(\omega) = -\frac{j}{C\omega}$
Inductance 	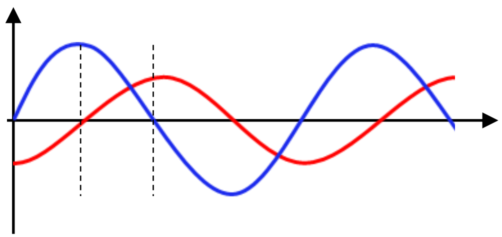	$\varphi = +\frac{\pi}{2}$ Current lags behind the voltage	$\tilde{Z}(\omega) = jL\omega$

I) Fundamentals of EIS

4) The RC element

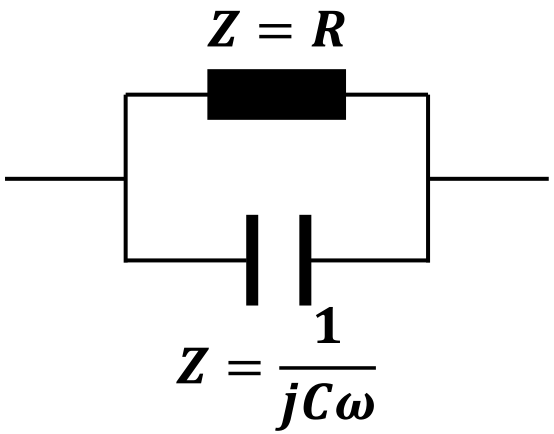

$$\frac{1}{Z} = \frac{1}{R} + jC\omega = \frac{1 + jRC\omega}{R}$$

$$Z = \frac{R}{1 + jRC\omega} = \frac{R - jR^2C\omega}{1 + (RC\omega)^2}$$

$$Z = \frac{R}{1 + (RC\omega)^2} - j\frac{R^2C\omega}{1 + (RC\omega)^2}$$

I) Fundamentals of EIS

5) Representing EIS data

$$Z = \frac{R}{1+(RC\omega)^2} - j\frac{R^2C\omega}{1+(RC\omega)^2}$$

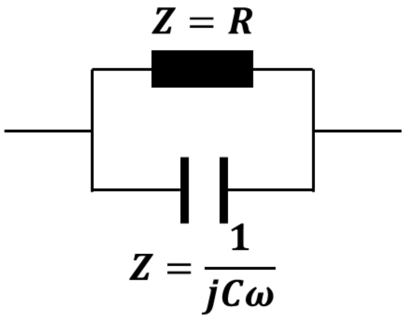

Bode Plots

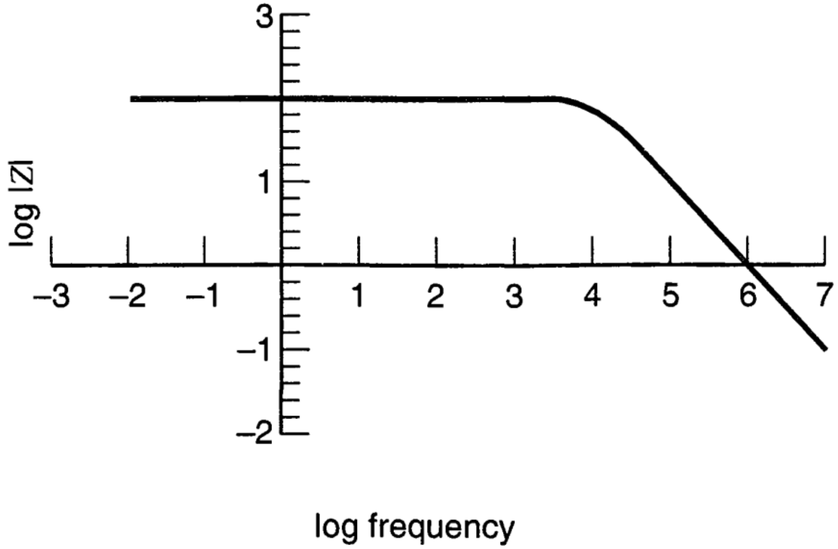

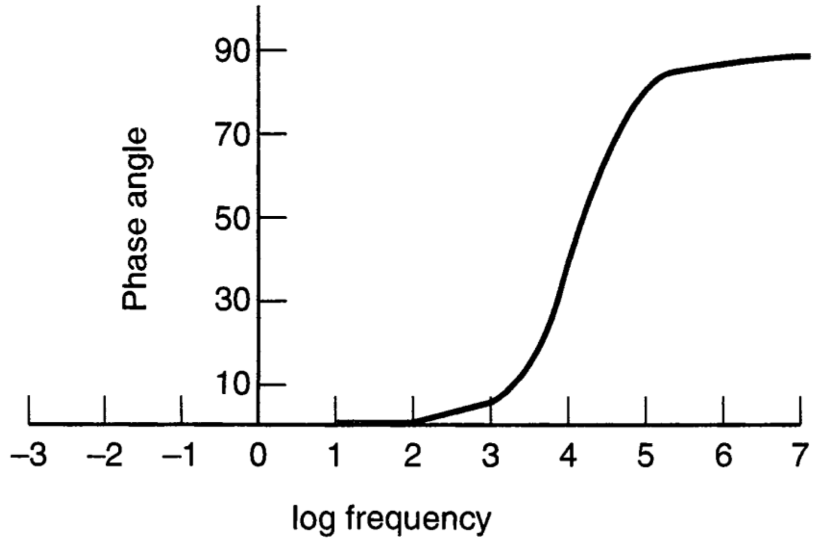

I) Fundamentals of EIS

5) Representing EIS data

$$Z = \frac{R}{1+(RC\omega)^2} - j\frac{R^2C\omega}{1+(RC\omega)^2}$$

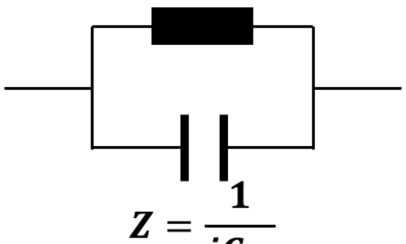

Nyquist Plots

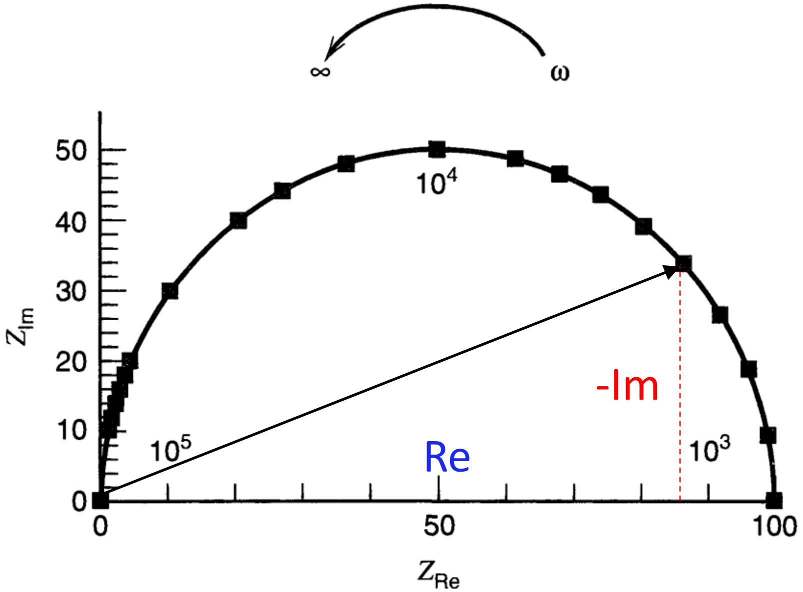

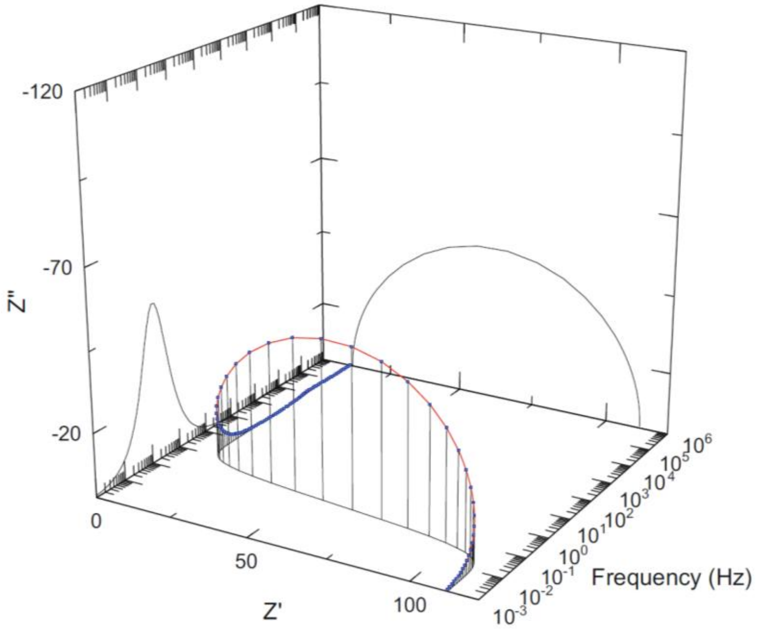

I) Fundamentals of EIS

6) Treatment of a ZARC element

$$Z = \frac{R}{1+(RC\omega)^2} - j\frac{R^2C\omega}{1+(RC\omega)^2}$$

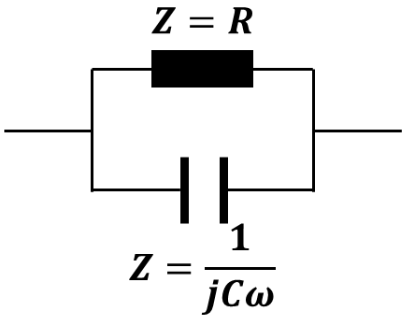

Nyquist Plots

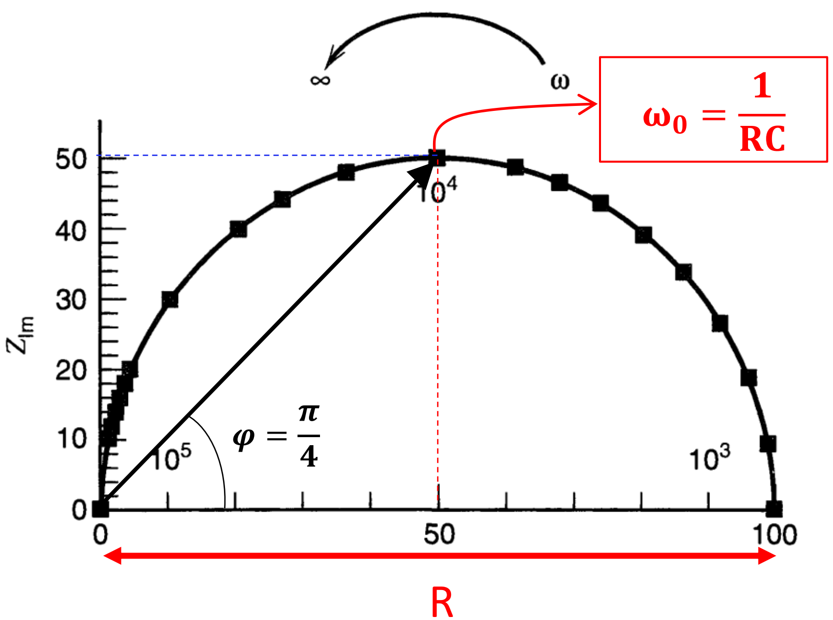

<u>Distinctive values:</u>

$$Z(\omega \mapsto \infty) = 0$$

$$Z(\omega \mapsto 0) = Z_{Re} = R$$

$$Z_{Re}(\omega_0) = -Z_{Im}(\omega_0) \Longrightarrow \omega_0 = \frac{1}{RC}$$

I) Fundamentals of EIS

7) Faradaic reaction: the Randles circuit

Ideally polarisable electrode

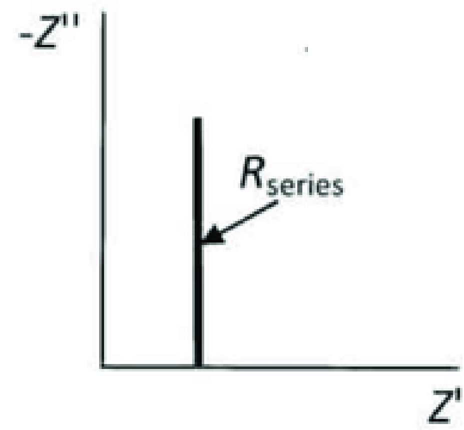

Electrolyte resistance R_E

Electrical double layer capacitance: C_{dl}

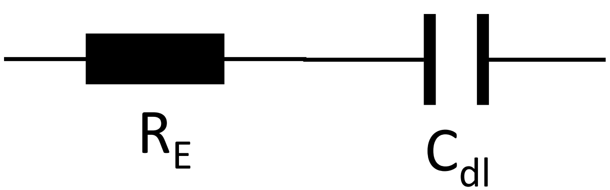

$$Z = R_E - j\frac{1}{C_{dl}\omega}$$

I) Fundamentals of EIS

7) Faradaic reaction: the Randles circuit

Charge transfer reaction

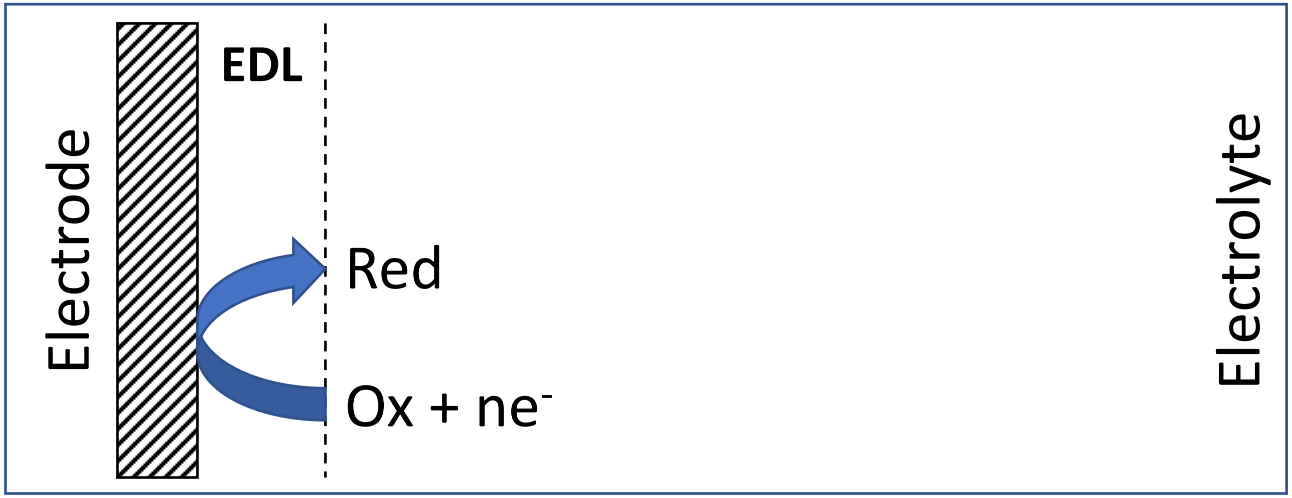

Prerequisites:

The system is linear

Ox and Red do not modify the electrode

High frequency ↔ no mass transfer limitation

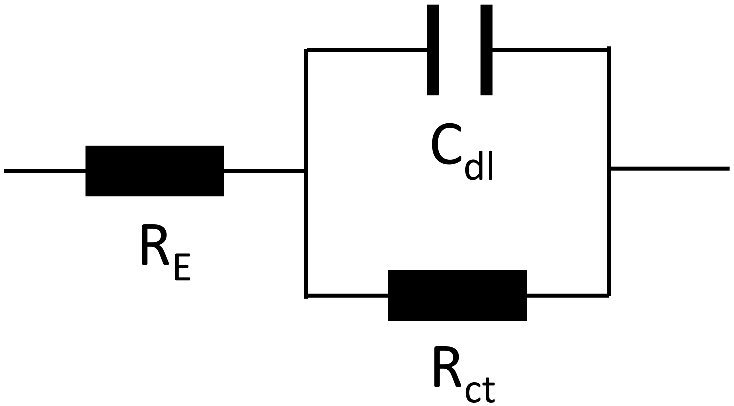

Electrolyte resistance R_E

Electrical double layer capacitance: C_{dl}

Charge transfer resistance R_{ct}

$$Z = R_E + \frac{R_{ct}}{1+(R_{ct}C_{dl}\omega)^2} - j\frac{{R_{ct}}^2 C_{dl}\omega}{1+(R_{ct}C_{dl}\omega)^2}$$

I) Fundamentals of EIS

7) Faradaic reaction: the Randles circuit

Charge transfer reaction

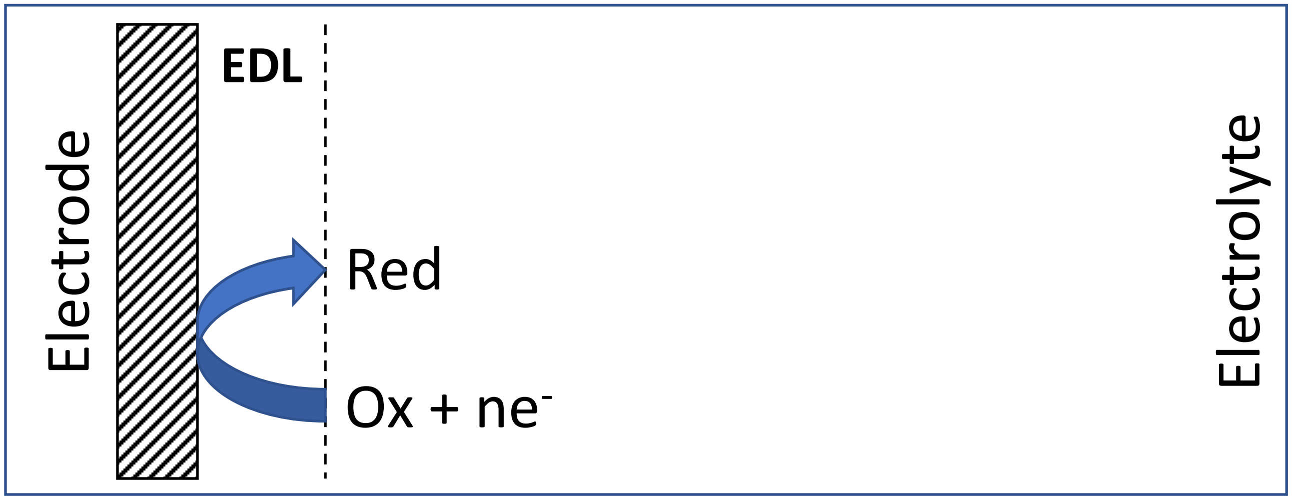

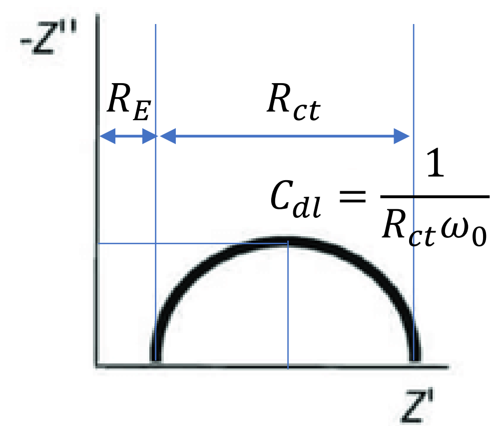

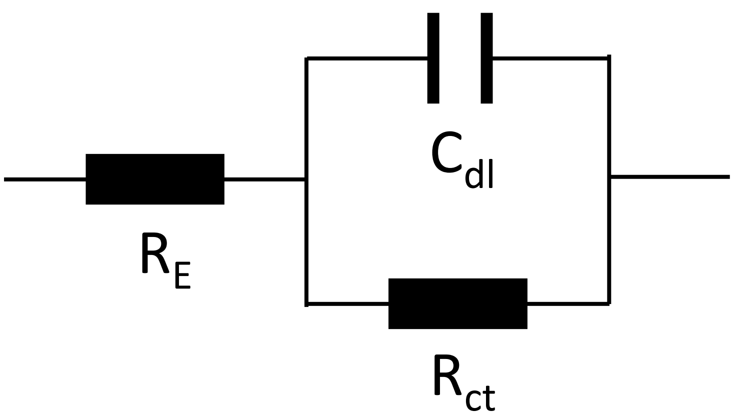

Electrolyte resistance R_E

Electrical double layer capacitance: C_{dl}

Charge transfer resistance R_{ct}

$$Z = R_E + \frac{R_{ct}}{1 + (R_{ct}C_{dl}\omega)^2} - j\frac{{R_{ct}}^2 C_{dl}\omega}{1 + (R_{ct}C_{dl}\omega)^2}$$

I) Fundamentals of EIS

7) Faradaic reaction: the Randles circuit

Charge transfer reaction

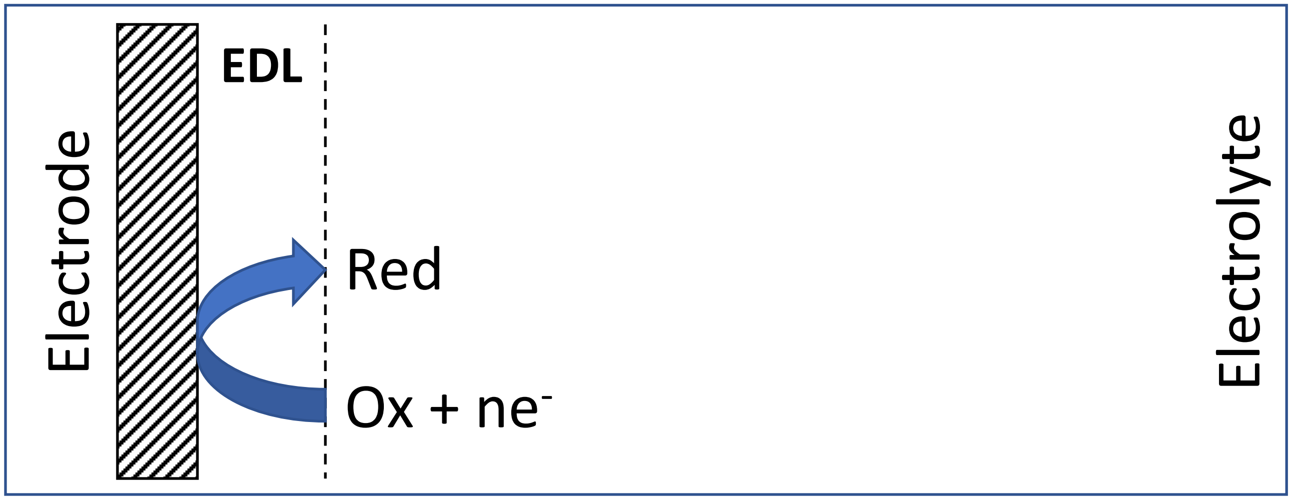

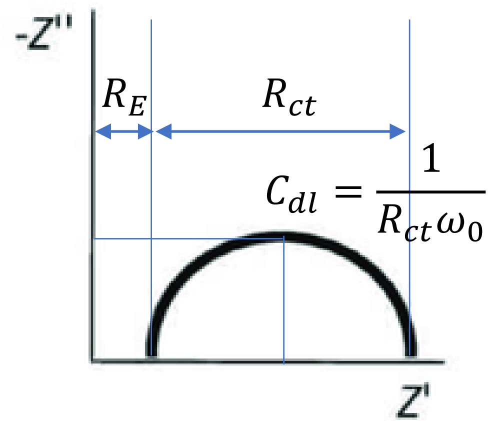

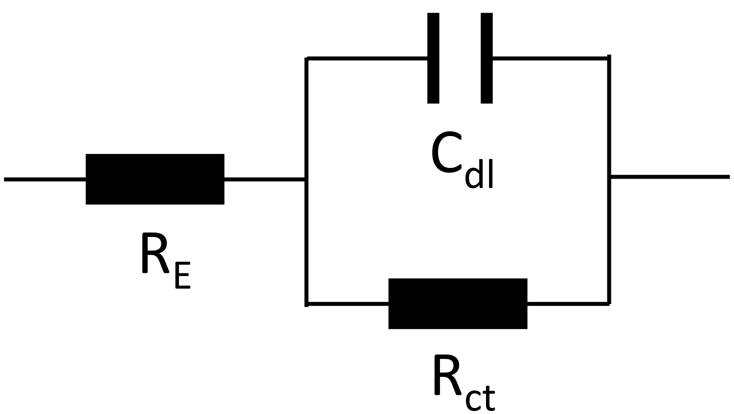

Low η: linearized Butler-Volmer $i = i_0 \cdot \frac{zF\eta}{RT}$

hence $R_{ct} = \frac{RT}{zFi_0} \Leftrightarrow i_0 = \frac{RT}{zFR_{ct}}$

$$i_0 = zF[Ox]\beta_{Red} \cdot exp^{\frac{-\Delta G^*_{\chi,\,Red}}{RT}} \cdot exp^{\frac{-\alpha zF\Delta\phi_{eq}}{RT}}$$

$$= zF[Red]\beta_{Ox} \cdot exp^{\frac{-\Delta G^*_{\chi,\,Ox}}{RT}} \cdot exp^{\frac{(1-\alpha)zF\Delta\phi_{eq}}{RT}}$$

I) Fundamentals of EIS

7) Faradaic reaction: the Randles circuit

Charge transfer reaction

Measure R_{ct} at different temperatures: Arrhenius plot

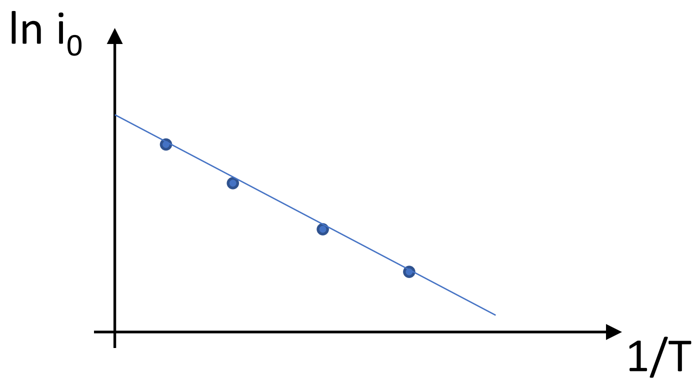

$$\ln i_0 = -\frac{\Delta G^*_{\chi,Red} + \alpha z F \Delta\phi_{eq}}{RT} + \ln(zF[Ox]\beta_{Red})$$

$$\ln i_0 = -\frac{\Delta G^*_{\chi,Ox} + (1-\alpha) z F \Delta\phi_{eq}}{RT} + \ln(zF[Red]\beta_{Ox})$$

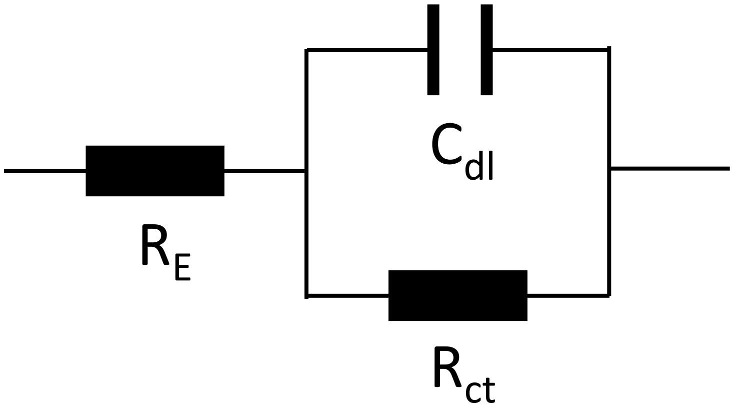

Low η: linearized Butler-Volmer $i = i_0 \cdot \frac{zF\eta}{RT}$

hence $R_{ct} = \frac{RT}{zFi_0} \Leftrightarrow i_0 = \frac{RT}{zFR_{ct}}$

$$i_0 = zF[Ox]\beta_{Red} \cdot exp^{\frac{-\Delta G^*_{\chi,Red}}{RT}} \cdot exp^{\frac{-\alpha zF\Delta\phi_{eq}}{RT}}$$

$$= zF[Red]\beta_{Ox} \cdot exp^{\frac{-\Delta G^*_{\chi,Ox}}{RT}} \cdot exp^{\frac{(1-\alpha)zF\Delta\phi_{eq}}{RT}}$$

I) Fundamentals of EIS

7) Faradaic reaction: the Randles circuit

$[Ox]^{el}$ and $[Red]^{el}$ are time dependent

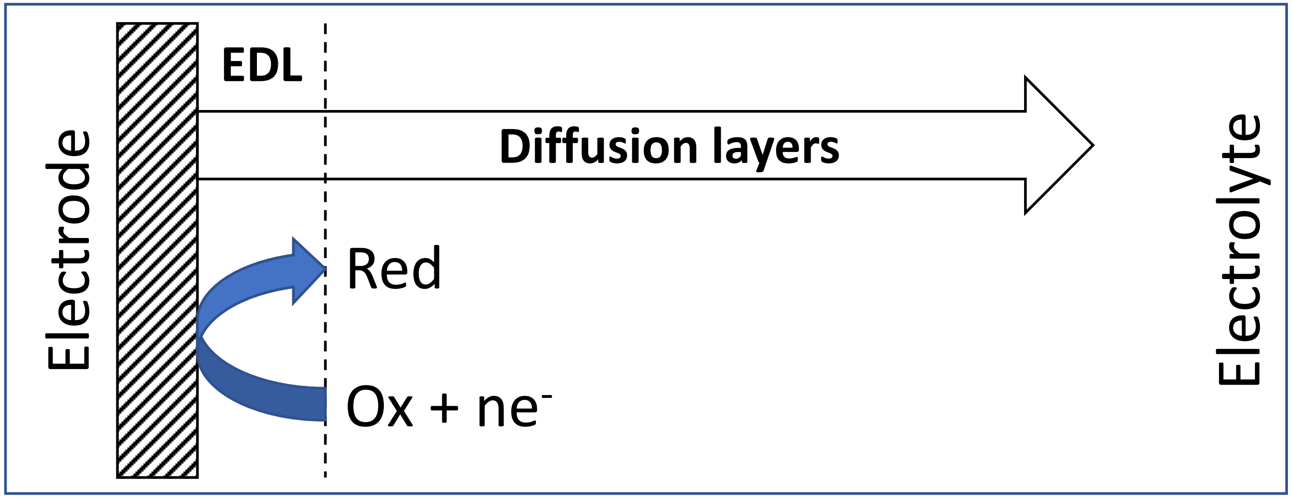

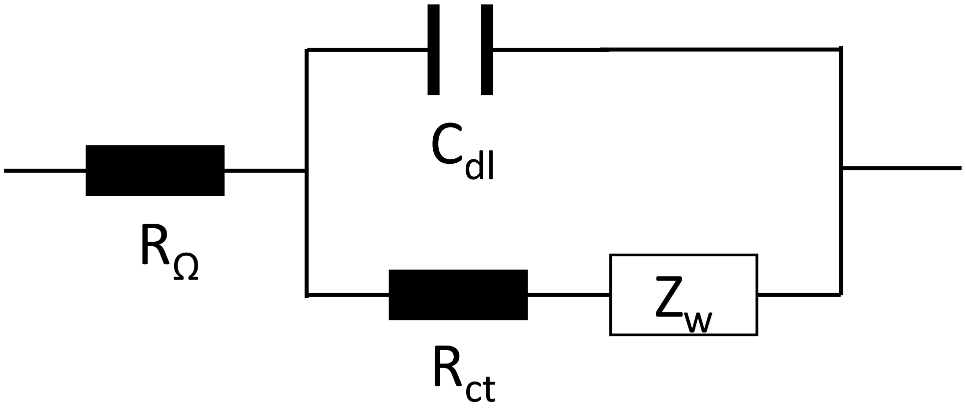

Ohmic resistance of the circuit $R_Ω$

Electrical double layer capacitance: C_{dl}

Charge transfer resistance R_{ct}

Warburg Impedance Z_w for diffusion

I) Fundamentals of EIS

7) Faradaic reaction: the Randles circuit

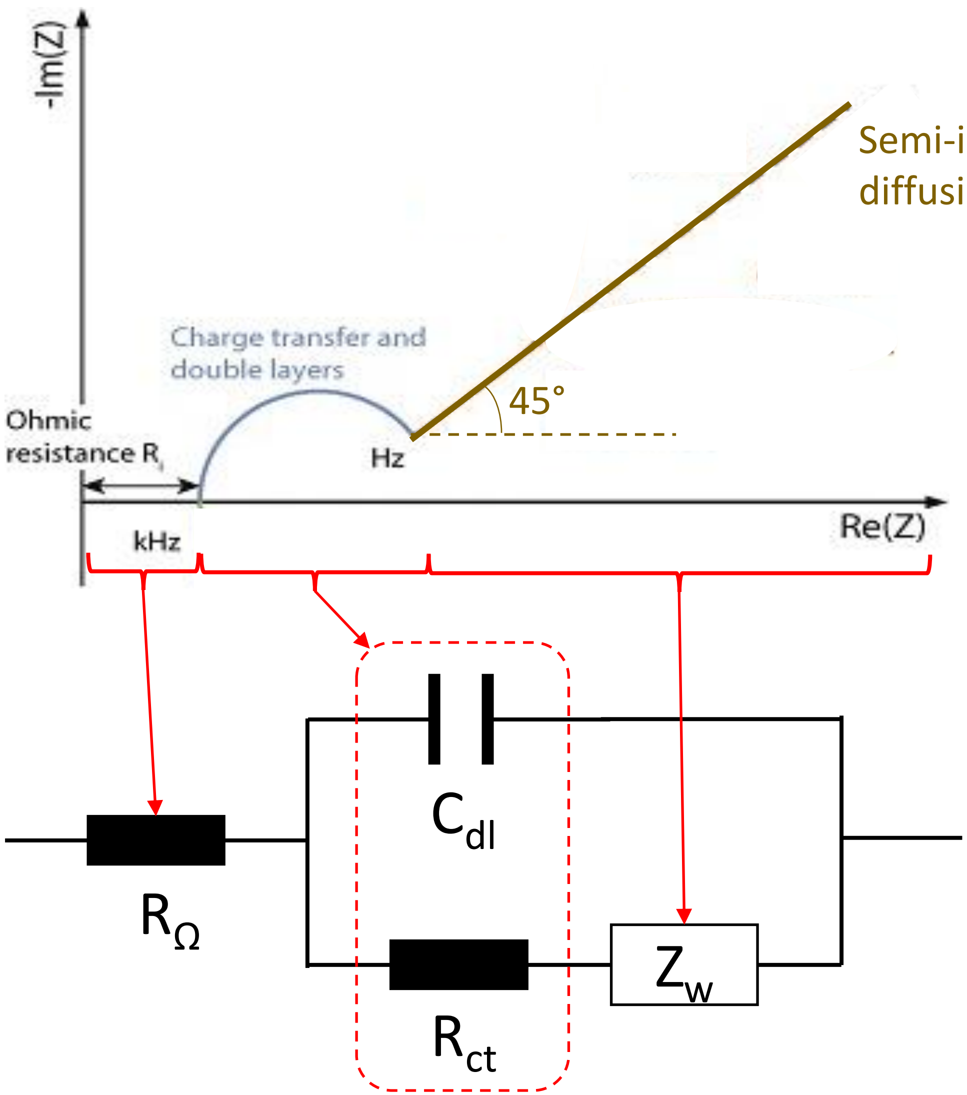

Ohmic resistance of the circuit R_{Ω}

Electrical double layer capacitance: C_{dl}

Charge transfer resistance R_{ct}

Warburg Impedance Z_w for diffusion

I) Fundamentals of EIS

7) Faradaic reaction: the Randles circuit

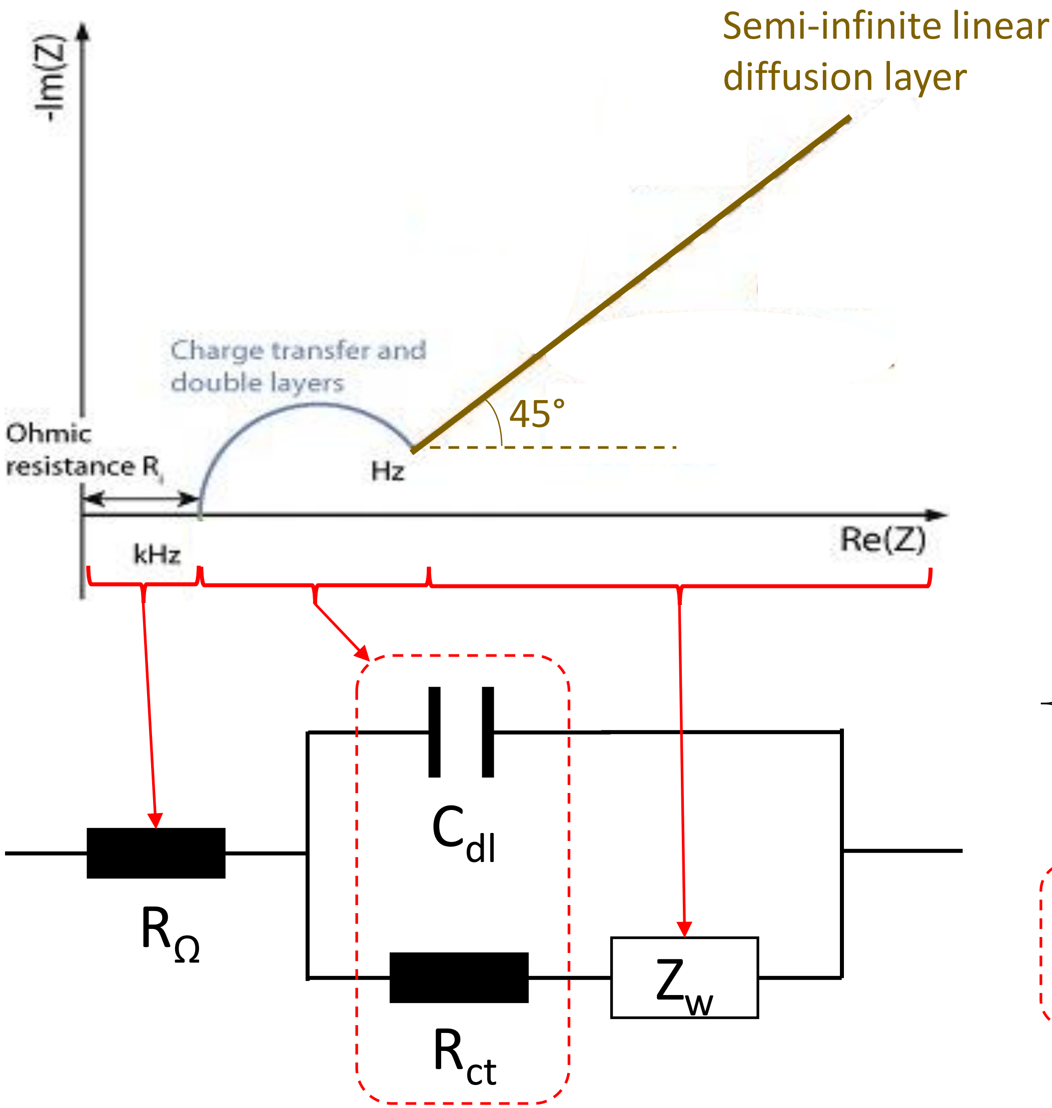

Butler-Volmer with mass limitation:

$$\tilde{i} = i_0\left(\frac{\widetilde{C_R}}{C_R{}^0}\, exp^{\frac{(1-\alpha)zF\tilde{\eta}}{RT}} - \frac{\widetilde{C_O}}{C_O{}^0}\, exp^{\frac{-\alpha zF\tilde{\eta}}{RT}}\right)$$

Fick's 2nd law of diffusion:

$$\frac{\partial C_i}{\partial t} = D_i \frac{\partial^2 C_i}{\partial x^2}$$

with $C_i(t) = C_i{}^{DC} + C_i{}^{AC} exp^{j(\omega t + \varphi_i)}$

Boundary conditions:

$$\left[\begin{aligned} & x \mapsto 0 \Longrightarrow \tilde{i} = zFD_i \frac{d\widetilde{C_i}}{dx} \\ & x \mapsto \infty \Longrightarrow C_i = C_i{}^0 \\ & D_R \frac{dC_R}{dx} = -D_O \frac{dC_O}{dx} \end{aligned}\right] \quad \widetilde{C_i} = \frac{\tilde{i}}{zF\sqrt{j\omega D_i}}\, exp^{-\sqrt{\frac{j\omega}{D_i}}x}$$

$$Z_W{}^{\infty} = \frac{\tilde{E}}{\tilde{i}} = \frac{1-j}{\sqrt{\omega}} \cdot \frac{RT}{\sqrt{2}(zF)^2}\left\{\frac{1}{C_O{}^0\sqrt{D_O}} + \frac{1}{C_R{}^0\sqrt{D_R}}\right\}$$

I) Fundamentals of EIS

7) Faradaic reaction: the Randles circuit

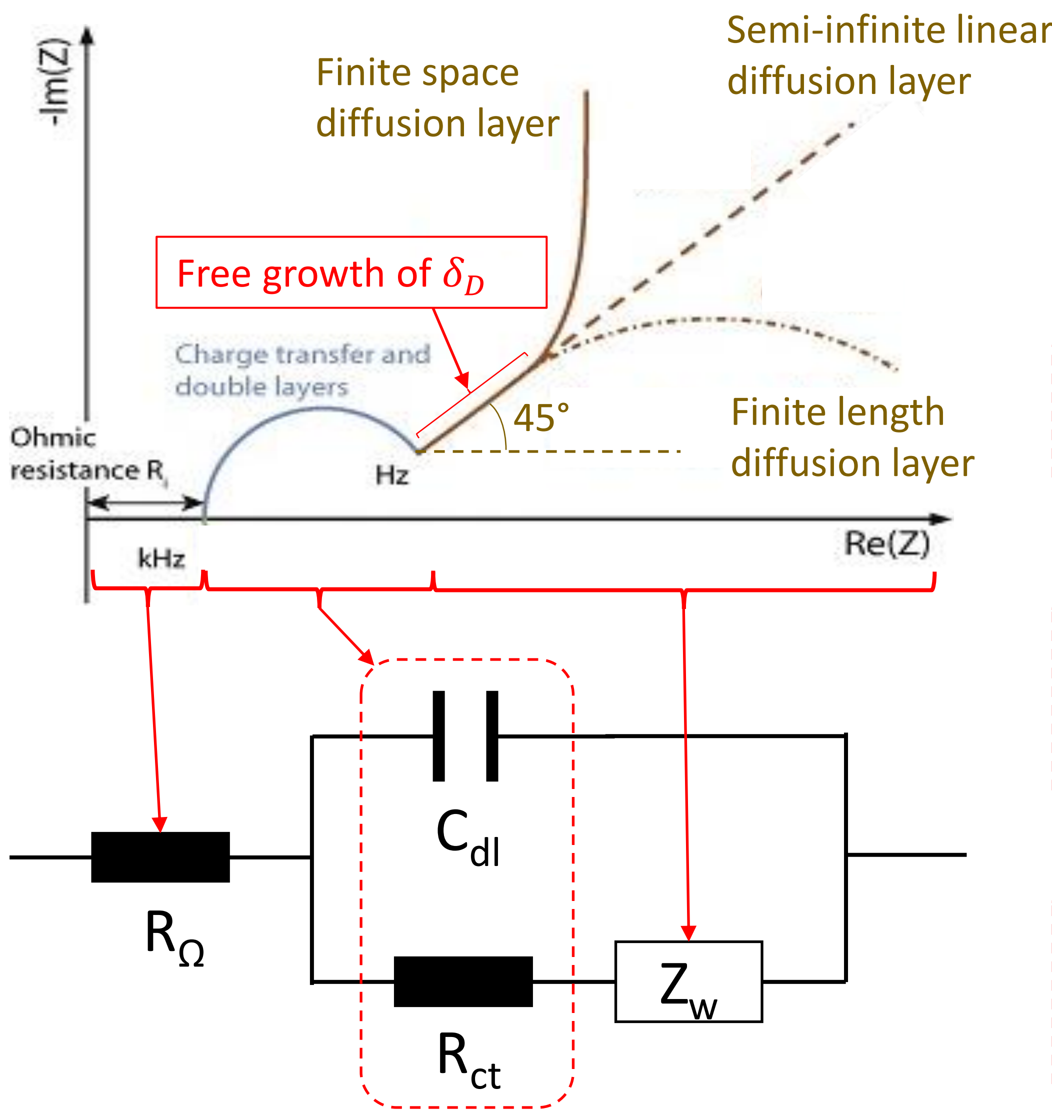

Initial boundary conditions:

$$\begin{cases} x \mapsto 0 \implies \tilde{\imath} = zFD_i \dfrac{d\widetilde{C}_i}{dx} \\ D_R \dfrac{dC_R}{dx} = -D_O \dfrac{dC_O}{dx} \end{cases}$$

Semi-infinite δ_D: $x \mapsto \infty \implies C_i = C_i^{\,0}$

$$Z_W^{\ \infty} = \frac{1-j}{\sqrt{\omega}} \cdot \frac{RT}{\sqrt{2}(zF)^2} \left\{ \frac{1}{C_O^{\,0}\sqrt{D_O}} + \frac{1}{C_R^{\,0}\sqrt{D_R}} \right\}$$

Finite space δ_D: $x = l \implies \dfrac{dC_i}{dx} = 0$

$$Z_W^{\ FS} = \frac{1-j}{\sqrt{\omega}} \cdot \frac{RT}{\sqrt{2}(zF)^2} \left\{ \frac{coth\sqrt{\frac{j\omega l}{D_O}}}{C_O^{\,0}\sqrt{D_O}} + \frac{coth\sqrt{\frac{j\omega l}{D_R}}}{C_R^{\,0}\sqrt{D_R}} \right\}$$

Finite length δ_D: $x = l \implies \delta_D = \delta_D^{\ max}$

$$Z_W^{\ FS} = \frac{1-j}{\sqrt{\omega}} \cdot \frac{RT}{\sqrt{2}(zF)^2} \left\{ \frac{tanh\sqrt{\frac{j\omega l}{D_O}}}{C_O^{\,0}\sqrt{D_O}} + \frac{tanh\sqrt{\frac{j\omega l}{D_R}}}{C_R^{\,0}\sqrt{D_R}} \right\}$$

I) Fundamentals of EIS

8) Constant phase element (CPE)

The Electrical Double Layer is not an ideal capacitor

There are distributed elements at the electrode/electrolyte interphase

$$Z_Q = \frac{1}{Q(j\omega)^{\alpha}} \quad with \quad 0 \le \alpha \le 1$$

$$Z_{ZARC} = \frac{R}{(1 + RQ(j\omega)^{\alpha})}$$

$$\alpha = \frac{2\chi}{\Pi}$$

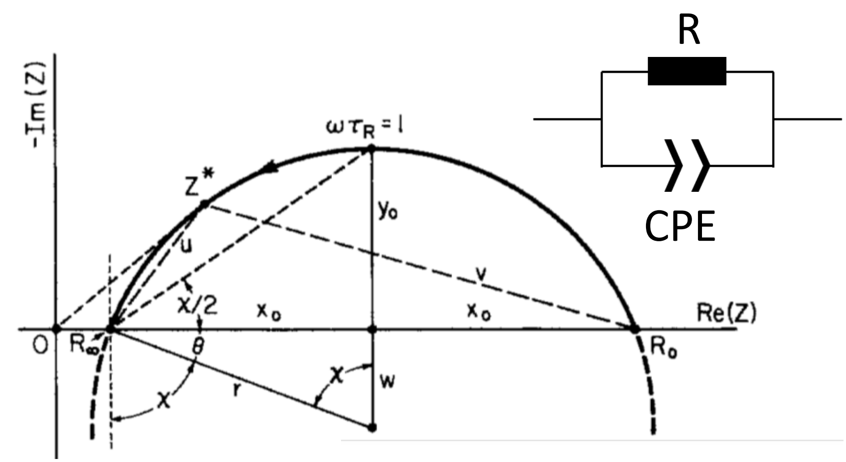

Dispersion of the relaxation frequency ↗ as α ↘

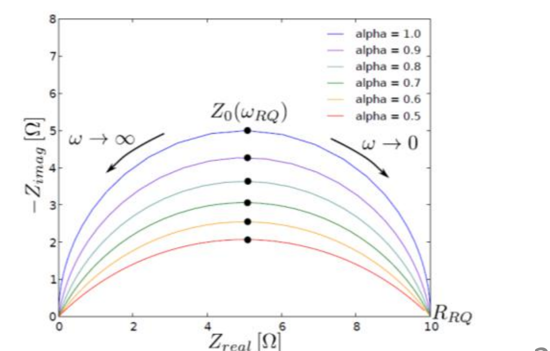

I) Fundamentals of EIS

8) Constant phase element (CPE)

The Electrical Double Layer is not an ideal capacitor

There are distributed elements at the electrode/electrolyte interphase

$$Z_Q = \frac{1}{Q(j\omega)^\alpha} \quad with \quad 0 \le \alpha \le 1$$

$$Z_{ZARC} = \frac{R}{(1 + RQ(j\omega)^\alpha)}$$

$$\alpha = \frac{2\chi}{\Pi}$$

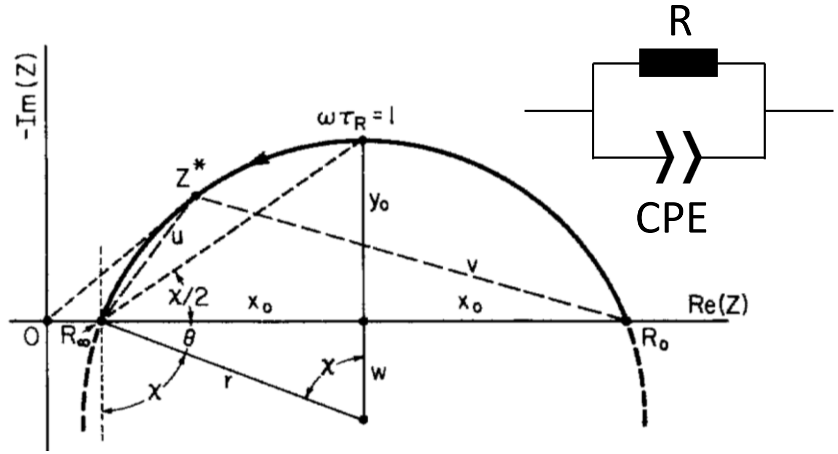

$$Re = \frac{R + \omega^\alpha R^2 Q \cos\left(\frac{\alpha}{2}\pi\right)}{1 + 2\omega^\alpha RQ \cos\left(\frac{\alpha}{2}\pi\right) + (\omega^\alpha RQ)^2}$$

$$Im = \frac{-\omega^\alpha R^2 Q \sin\left(\frac{\alpha}{2}\pi\right)}{1 + 2\omega^\alpha RQ \cos\left(\frac{\alpha}{2}\pi\right) + (\omega^\alpha RQ)^2}$$

I) Fundamentals of EIS

8) Transmission lines:
De Levie model for porous media

A conductive pore in an ionic conductor

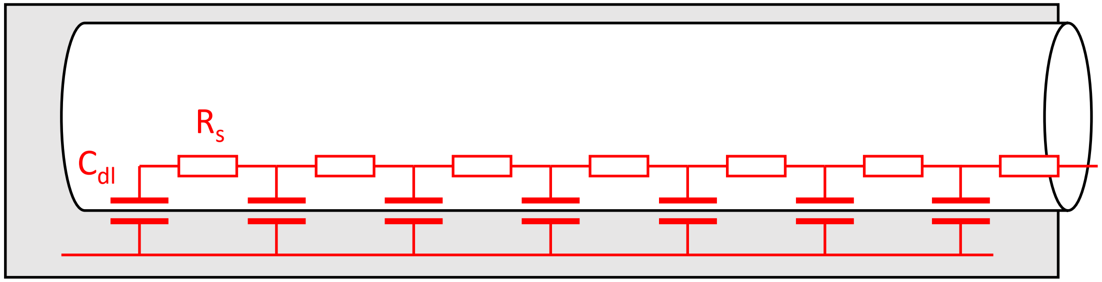

$$\widetilde{E} = \widetilde{E}_0 \frac{\cosh\left[\sqrt{\frac{r_s}{\hat{z}}}(l-x)\right]}{\cosh\left[\sqrt{\frac{r_s}{\hat{z}}}\,l\right]}.$$

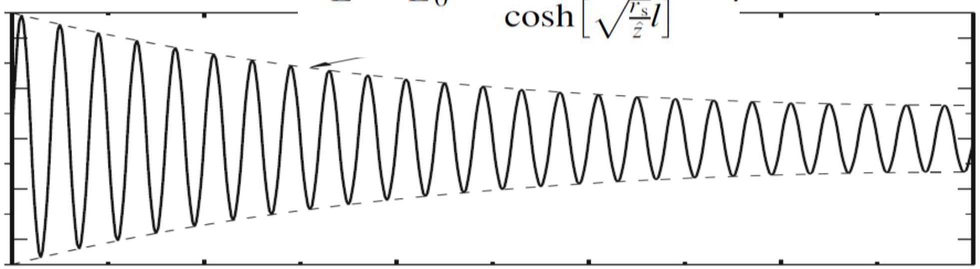

$$\hat{Z}_{\text{pore}} = \frac{R_{\Omega,p}}{\Lambda^{1/2}} \coth\left(\Lambda^{1/2}\right)$$

$$\Lambda = \frac{r_S l^2}{\hat{z}} = \frac{2\rho_s l^2}{r\hat{Z}_{\text{el}}} = \frac{2\rho_s l^2 j\omega C_{\text{dl}}}{r}$$

I) Fundamentals of EIS

element	impedance	process
(R) serial resistor	R	contact and electrolyte resistance
(RQ) resistor and a constant phase element in parallel	$\frac{R}{1+RQ_0(j\omega)^n}$	double layer capacitance and charge-transfer reactions in parallel
(G) Gerischer element	$\frac{R_{\text{chem}}}{\sqrt{1+j\omega t_{\text{chem}}}}$	combination of electrochemical charge-transfer and diffusion
(W) Warburg element	$R_{\text{W}}\frac{\tanh[(j\omega T)^\alpha]}{(j\omega T)^\alpha}$	diffusion processes
(TLM) transition line model	$\frac{R_{\text{el}}R_{\text{ion,L}}}{R_{\text{el}}+R_{\text{ion,L}}}\left(L+\frac{2\lambda}{\sinh(L/\lambda)}\right)+ \lambda_{TLM}\frac{R_{\text{el}}^2+R_{\text{ion,L}}^2}{R_{\text{el}}+R_{\text{ion,L}}}\coth\left(\frac{L}{\lambda_{\text{TLM}}}\right)$	porous electrode electrochemistry

II) Practical aspects, analyses, and applications

1) Impedance measurements

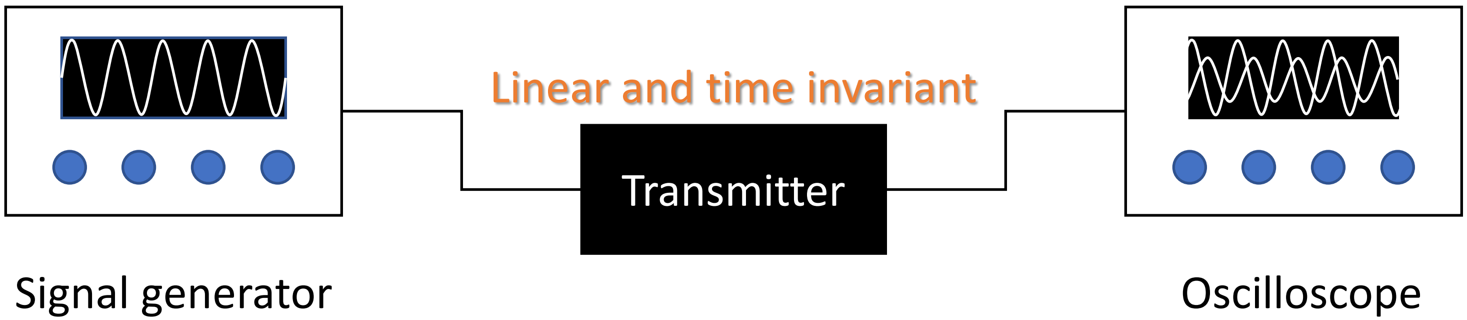

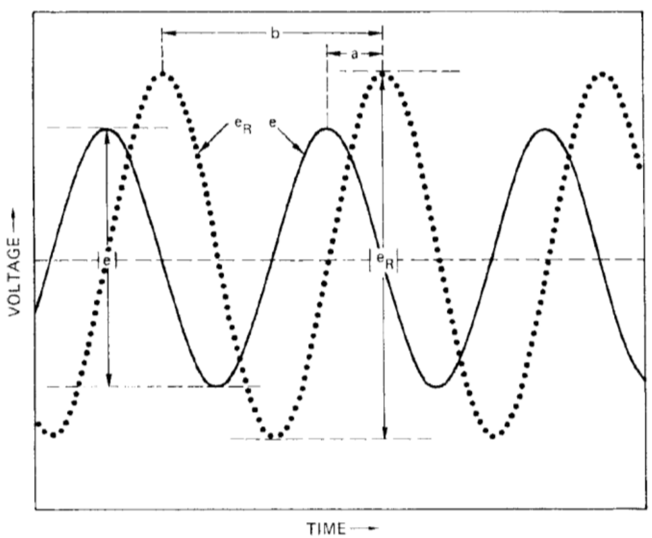

Measure f, i_{DC}, E_{DC}, Δi, and ΔE

Visual control of harmonics

To ensure the system linearity, we typically target $\Delta E \approx 10$ mV

II) Practical aspects, analyses, and applications

1) Impedance measurements

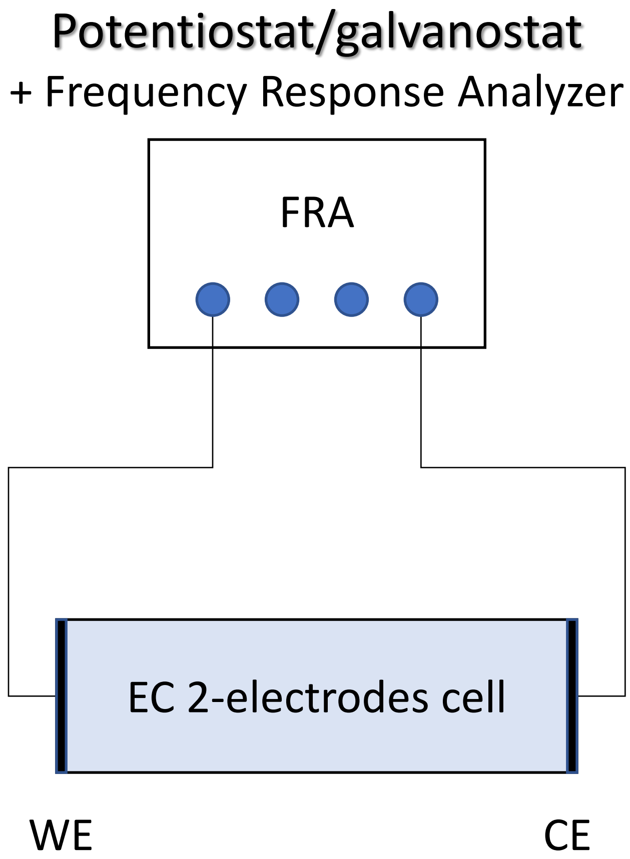

Possible to measure a 2-electrodes EC-cell

Complex equivalent circuit
- difficult to interpret
- deconvolute processes
- parametric study necessary

II) Practical aspects, analyses, and applications

1) Impedance measurements

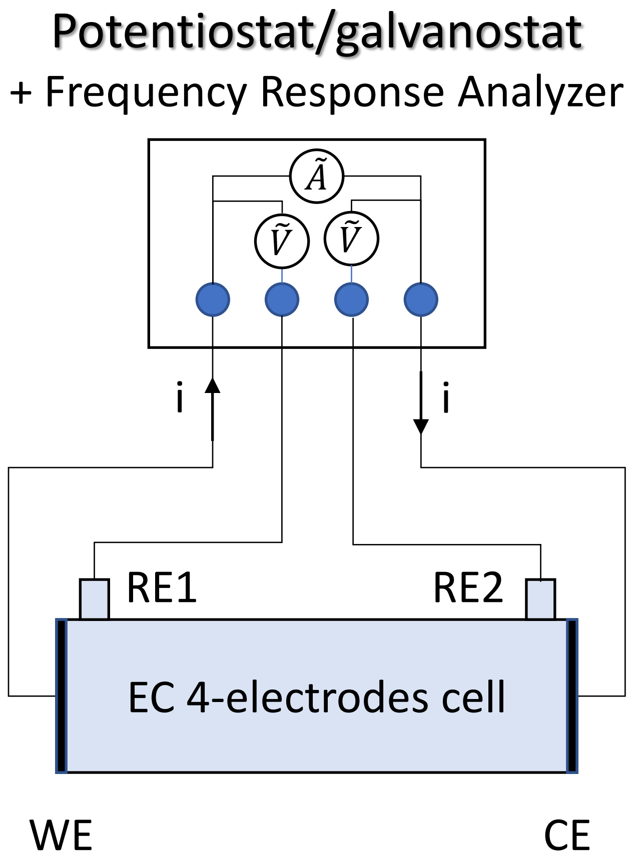

4-electrodes EC-cell easier to interpret

Separation of cathodic and anodic elements

II) Practical aspects, analyses, and applications

1) Impedance measurements

Suppressing the wire inductance

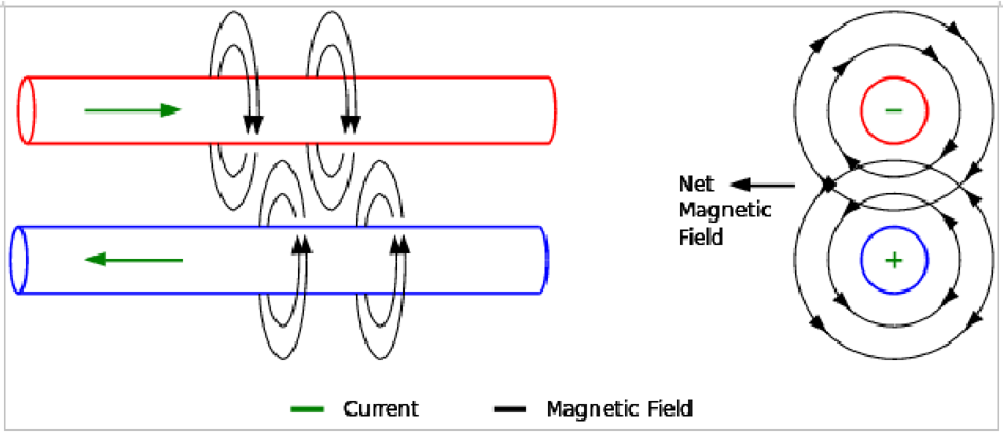

Wire inductance results from opposite currents flowing through parallel wires

Compensation of inductive currents by uniform twisting of the wires

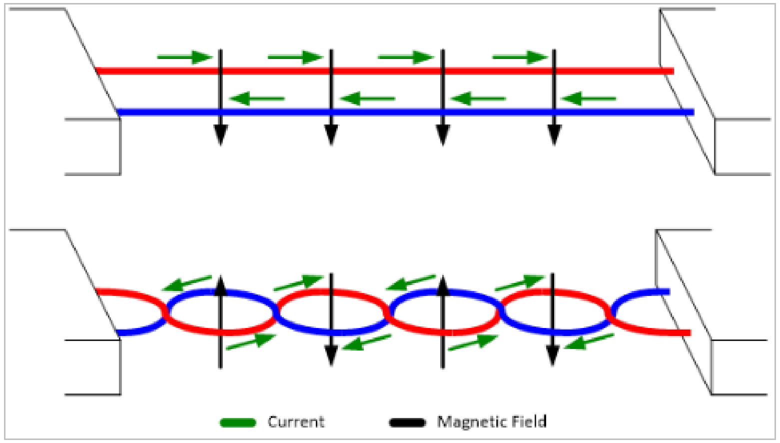

II) Practical aspects, analyses, and applications

2) Data treatment

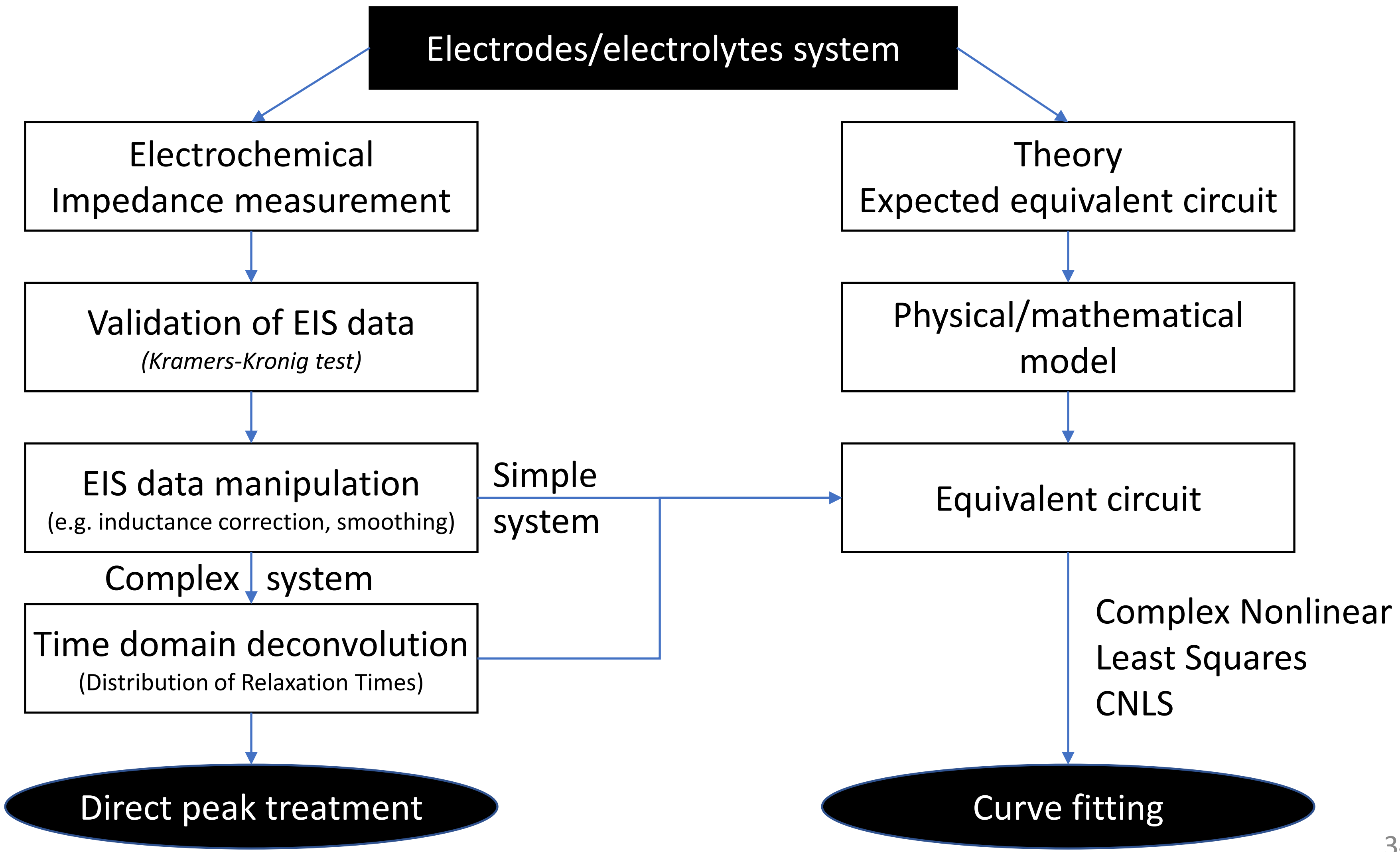

II) Practical aspects, analyses, and applications

2) Data treatment

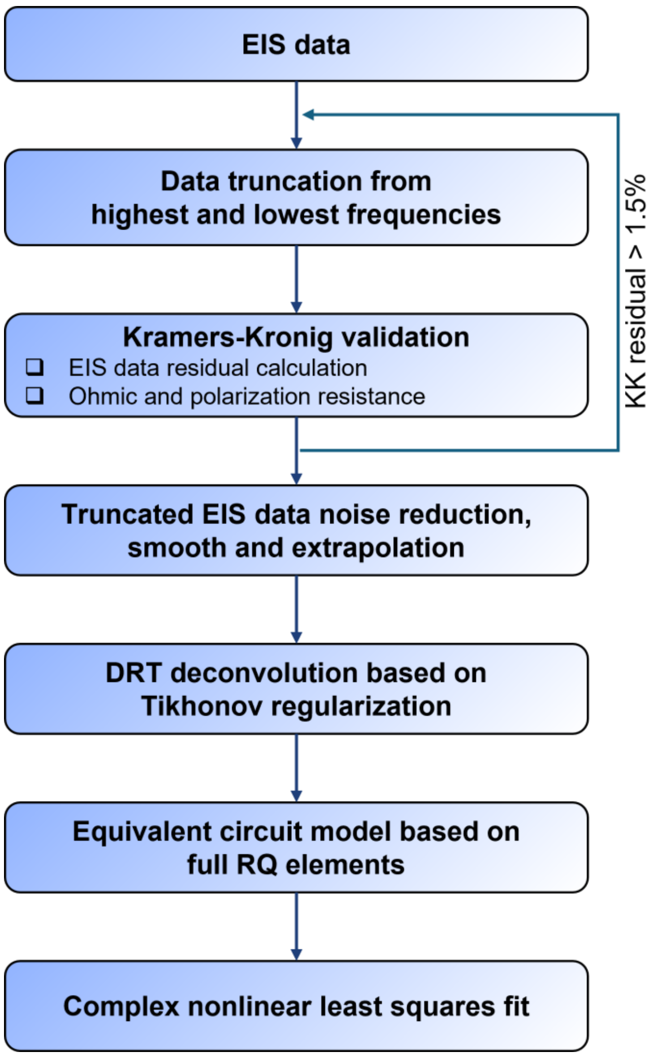

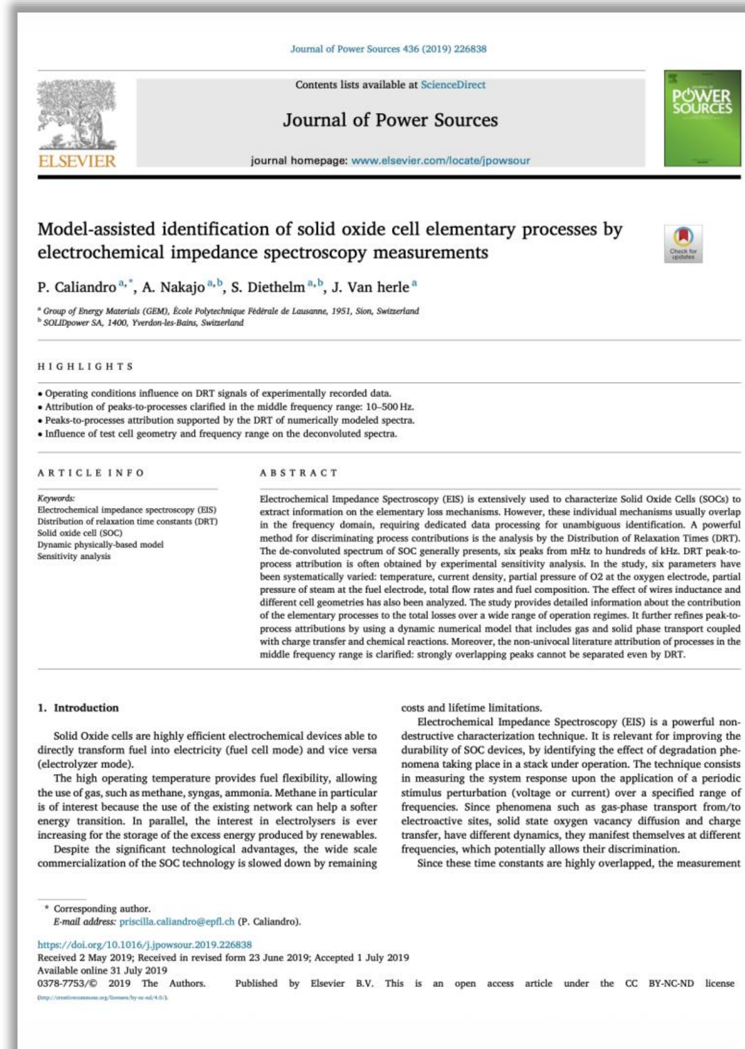

Journal of Power Sources 436 (2019) 226838

Contents lists available at ScienceDirect

Journal of Power Sources

journal homepage: www.elsevier.com/locate/jpowsour

Model-assisted identification of solid oxide cell elementary processes by electrochemical impedance spectroscopy measurements

P. Caliandro [a,*], A. Nakajo [a,b], S. Diethelm [a,b], J. Van herle [a]

[a] Group of Energy Materials (GEM), École Polytechnique Fédérale de Lausanne, 1951, Sion, Switzerland
[b] SOLIDpower SA, 1400, Yverdon-les-Bains, Switzerland

H I G H L I G H T S

- Operating conditions influence on DRT signals of experimentally recorded data.
- Attribution of peaks-to-processes clarified in the middle frequency range: 10–500 Hz.
- Peaks-to-processes attribution supported by the DRT of numerically modeled spectra.
- Influence of test cell geometry and frequency range on the deconvoluted spectra.

A R T I C L E I N F O

Keywords:
Electrochemical impedance spectroscopy (EIS)
Distribution of relaxation time constants (DRT)
Solid oxide cell (SOC)
Dynamic physically-based model
Sensitivity analysis

A B S T R A C T

Electrochemical Impedance Spectroscopy (EIS) is extensively used to characterize Solid Oxide Cells (SOCs) to extract information on the elementary loss mechanisms. However, these individual mechanisms usually overlap in the frequency domain, requiring dedicated data processing for unambiguous identification. A powerful method for discriminating process contributions is the analysis by the Distribution of Relaxation Times (DRT). The de-convoluted spectrum of SOC generally presents, six peaks from mHz to hundreds of kHz. DRT peak-to-process attribution is often obtained by experimental sensitivity analysis. In the study, six parameters have been systematically varied: temperature, current density, partial pressure of O2 at the oxygen electrode, partial pressure of steam at the fuel electrode, total flow rates and fuel composition. The effect of wires inductance and different cell geometries has also been analyzed. The study provides detailed information about the contribution of the elementary processes to the total losses over a wide range of operation regimes. It further refines peak-to-process attributions by using a dynamic numerical model that includes gas and solid phase transport coupled with charge transfer and chemical reactions. Moreover, the non-univocal literature attribution of processes in the middle frequency range is clarified: strongly overlapping peaks cannot be separated even by DRT.

1. Introduction

Solid Oxide cells are highly efficient electrochemical devices able to directly transform fuel into electricity (fuel cell mode) and vice versa (electrolyzer mode).

The high operating temperature provides fuel flexibility, allowing the use of gas, such as methane, syngas, ammonia. Methane in particular is of interest because the use of the existing network can help a softer energy transition. In parallel, the interest in electrolysers is ever increasing for the storage of the excess energy produced by renewables.

Despite the significant technological advantages, the wide scale commercialization of the SOC technology is slowed down by remaining costs and lifetime limitations.

Electrochemical Impedance Spectroscopy (EIS) is a powerful non-destructive characterization technique. It is relevant for improving the durability of SOC devices, by identifying the effect of degradation phenomena taking place in a stack under operation. The technique consists in measuring the system response upon the application of a periodic stimulus perturbation (voltage or current) over a specified range of frequencies. Since phenomena such as gas-phase transport from/to electroactive sites, solid state oxygen vacancy diffusion and charge transfer, have different dynamics, they manifest themselves at different frequencies, which potentially allows their discrimination.

Since these time constants are highly overlapped, the measurement

* Corresponding author.
E-mail address: priscilla.caliandro@epfl.ch (P. Caliandro).

https://doi.org/10.1016/j.jpowsour.2019.226838
Received 2 May 2019; Received in revised form 23 June 2019; Accepted 1 July 2019
Available online 31 July 2019

Schönleber, M., Klotz, D. and Ivers-Tiffée, E., 2014. A method for improving the robustness of linear Kramers-Kronig validity tests. Electrochimica Acta, 131, pp.20-27.
Boukamp, B.A., 1995. A linear Kronig-Kramers transform test for immittance data validation. Journal of the electrochemical society, 142(6), p.1885.

II) Practical aspects, analyses, and applications

Kramers-Kronig Transform (Linearity test)

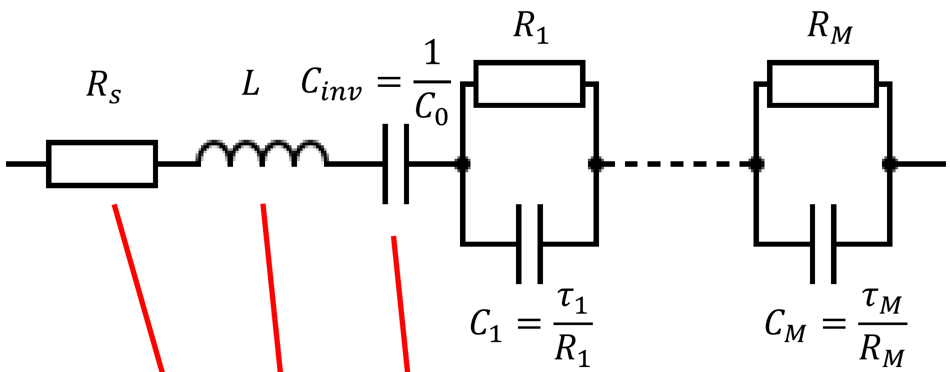

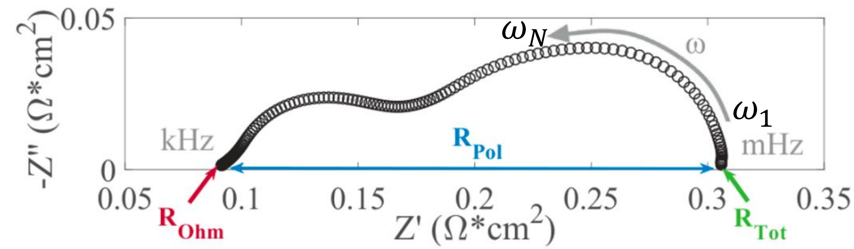

$$Z_{fit,i} = R_s + j\omega_i L + \frac{C_{inv}}{j\omega_i} + \sum_{k=1}^{M} \frac{R_k}{1+(\omega_i \tau_k)} = \left(R_s + \sum_{k=1}^{M} \frac{R_k}{1+(\omega_i \tau_k)^2}\right) + j \cdot \left(\omega_i L - \frac{C_{inv}}{\omega_i} - \sum_{k=1}^{M} \frac{R_k \omega_i \tau_k}{1+(\omega_i \tau_k)^2}\right)$$

$Re_{fit,i}$ $\quad$ $Im_{fit,i}$

$$Z_{fit} = \sum_{i=1}^{N} Z_{fit,i} = \sum_{i=1}^{N} (Re_{fit,i} + j \cdot IM_{fit,i})$$

$$Re_{fit} = \sum_{i=1}^{N} \left(R_s + \sum_{k=1}^{M} \frac{R_k}{1+(\omega_i \tau_k)^2}\right)$$

$$Im_{fit} = \sum_{i=1}^{N} \left(\omega_i L - \frac{C_{inv}}{\omega_i} - \sum_{k=1}^{M} \frac{R_k \omega_i \tau_k}{1+(\omega_i \tau_k)^2}\right)$$

$$\tau_k = R_k C_k = 10^{\log_{10}(\tau_{min}) + \frac{k-1}{M-1} \cdot [\log_{10}(\tau_{max}) - \log_{10}(\tau_{min})]}$$

$$S = \sum_{i=1}^{N} \lambda_i [(Re_i - Re_{fit,i})^2 + (Im_i - Im_{fit,i})^2]$$

Weight: $\lambda_i = \frac{1}{|Z_i|^2} = \frac{1}{Re_i^2 + Im_i^2}$

Objective: $\text{argmin} S \rightarrow \nabla S = 0 \rightarrow \frac{\delta S}{\delta R_j} = 0$

Unknown parameters: $X = [R_s, L, C_{inv}, R_1, R_2, \ldots, R_k]^T$

Schönleber, M., Klotz, D. and Ivers-Tiffée, E., 2014. A method for improving the robustness of linear Kramers-Kronig validity tests. Electrochimica Acta, 131, pp.20-27.
Boukamp, B.A., 1995. A linear Kronig-Kramers transform test for immittance data validation. Journal of the electrochemical society, 142(6), p.1885.

II) Practical aspects, analyses, and applications

Kramers-Kronig Transform (Linearity test)

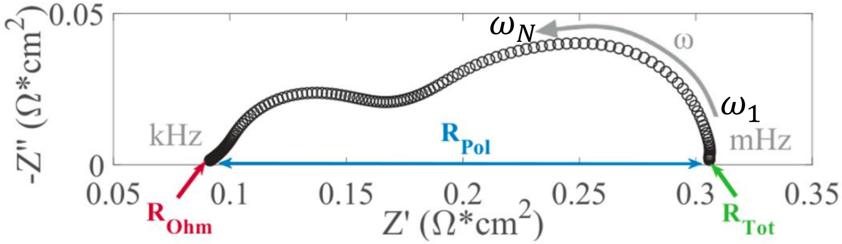

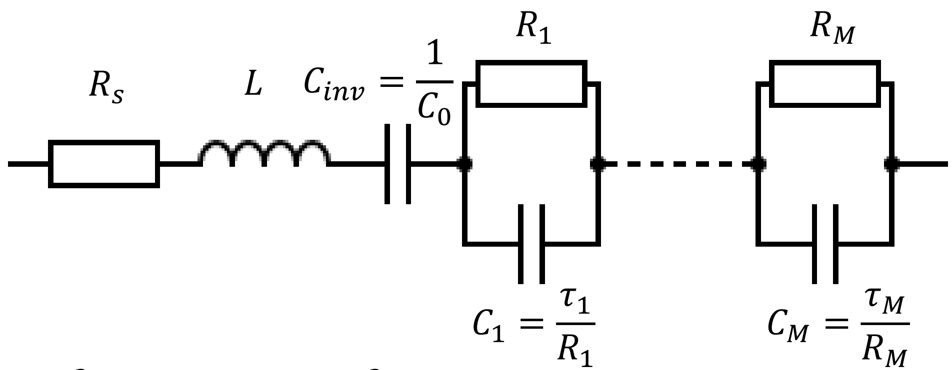

R_s as an example with $S = \sum_{i=1}^{N} \lambda_i[(Re_i - Re_{fit,i})^2 + (Im_i - Im_{fit,i})^2]$:

$$\frac{\delta S}{\delta R_s} = \sum_{i=1}^{N} [\lambda_i \cdot 2(Re_i - Re_{fit,i}) \cdot \frac{\delta Re_{fit,i}}{\delta R_s} + \lambda_i \cdot 2(Im_i - Im_{fit,i}) \cdot \frac{\delta Im_{fit,i}}{\delta R_s}]$$

$$\because Re_{fit,i} = R_s + \sum_{k=1}^{M} \frac{R_k}{1 + (\omega_i \tau_k)^2}, \qquad Im_{fit,i} = \omega_i L - \frac{C_{inv}}{\omega_i} - \sum_{k=1}^{M} \frac{R_k \omega_i \tau_k}{1 + (\omega_i \tau_k)^2}$$

$$\therefore \frac{\delta Re_{fit,i}}{\delta R_s} = 1, \qquad \frac{\delta Im_{fit,i}}{\delta R_s} = 0$$

$$\therefore \frac{\delta S}{\delta R_s} = \sum_{i=1}^{N} \lambda_i \cdot 2(Re_i - Re_{fit,i}) = 0$$

$$\therefore \sum_{i=1}^{N} \lambda_i Re_{fit,i} = \sum_{i=1}^{N} \lambda_i Re_i \Leftrightarrow R_s \sum_{i=1}^{N} \lambda_i + \sum_{k=1}^{M} R_k \sum_{i=1}^{N} \frac{\lambda_i}{1 + (\omega_i \tau_k)^2} = \sum_{i=1}^{N} \lambda_i Re_i \Leftrightarrow AX = b$$

Schönleber, M., Klotz, D. and Ivers-Tiffée, E., 2014. A method for improving the robustness of linear Kramers-Kronig validity tests. Electrochimica Acta, 131, pp.20-27.
Boukamp, B.A., 1995. A linear Kronig-Kramers transform test for immittance data validation. Journal of the electrochemical society, 142(6), p.1885.

II) Practical aspects, analyses, and applications

Kramers-Kronig Transform (Linearity test)

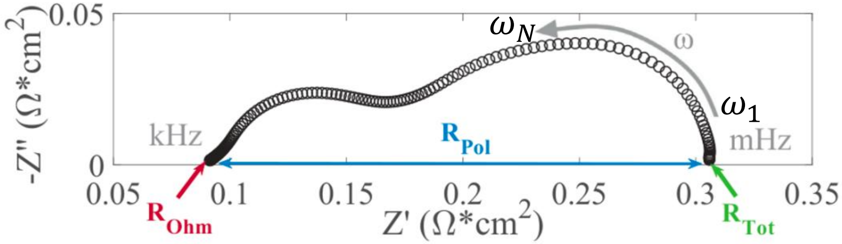

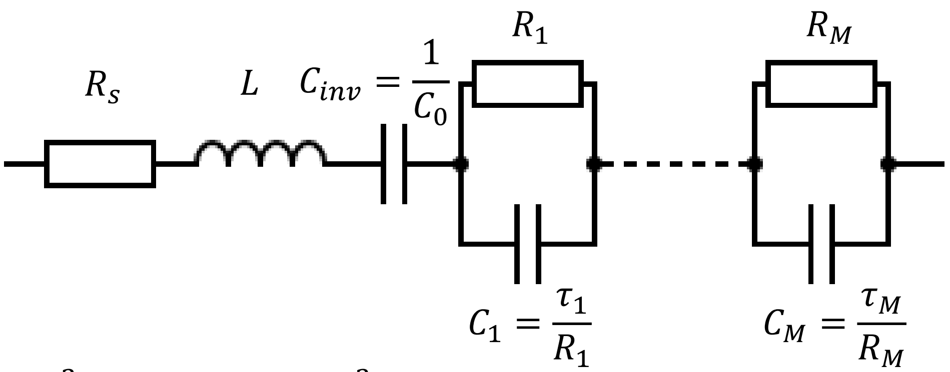

L as an example with $S = \sum_{i=1}^{N} \lambda_i [(Re_i - Re_{fit,i})^2 + (Im_i - Im_{fit,i})^2]$:

$$\frac{\delta S}{\delta L} = \sum_{i=1}^{N} [\lambda_i \cdot 2(Re_i - Re_{fit,i}) \cdot \frac{\delta Re_{fit,i}}{\delta L} + \lambda_i \cdot 2(Im_i - Im_{fit,i}) \cdot \frac{\delta Im_{fit,i}}{\delta L}]$$

$$\because Re_{fit,i} = R_s + \sum_{k=1}^{M} \frac{R_k}{1 + (\omega_i \tau_k)^2}, \qquad Im_{fit,i} = \omega_i L - \frac{C_{inv}}{\omega_i} - \sum_{k=1}^{M} \frac{R_k \omega_i \tau_k}{1 + (\omega_i \tau_k)^2}$$

$$\therefore \frac{\delta Re_{fit,i}}{\delta L} = 0, \qquad \frac{\delta Im_{fit,i}}{\delta L} = \omega_i$$

$$\therefore \frac{\delta S}{\delta L} = \sum_{i=1}^{N} \lambda_i \cdot 2\omega_i (Im_i - Im_{fit,i}) = 0$$

$$\therefore \sum_{i=1}^{N} \lambda_i \omega_i Im_{fit,i} = \sum_{i=1}^{N} \lambda_i \omega_i Im_i \Leftrightarrow \sum_{i=1}^{N} \lambda_i \omega_i L - \sum_{i=1}^{N} \frac{\lambda_i}{C_{inv}} - \sum_{k=1}^{M} R_k \sum_{i=1N} \frac{\omega_i^2 \tau_k}{1 + (\omega_i \tau_k)^2} = \sum_{i=1}^{N} \lambda_i \omega_i Im_i \Leftrightarrow AX = b$$

Schönleber, M., Klotz, D. and Ivers-Tiffée, E., 2014. A method for improving the robustness of linear Kramers-Kronig validity tests. Electrochimica Acta, 131, pp.20-27.
Boukamp, B.A., 1995. A linear Kronig-Kramers transform test for immittance data validation. Journal of the electrochemical society, 142(6), p.1885.

II) Practical aspects, analyses, and applications

Kramers-Kronig Transform (Linearity test)

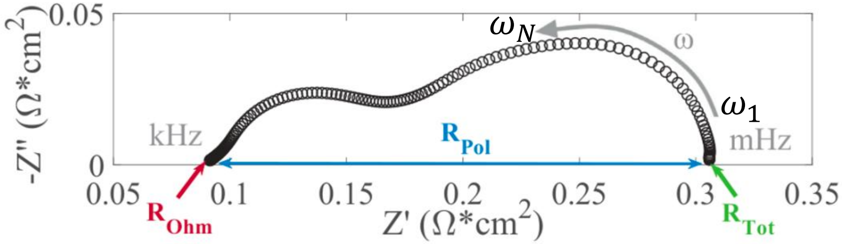

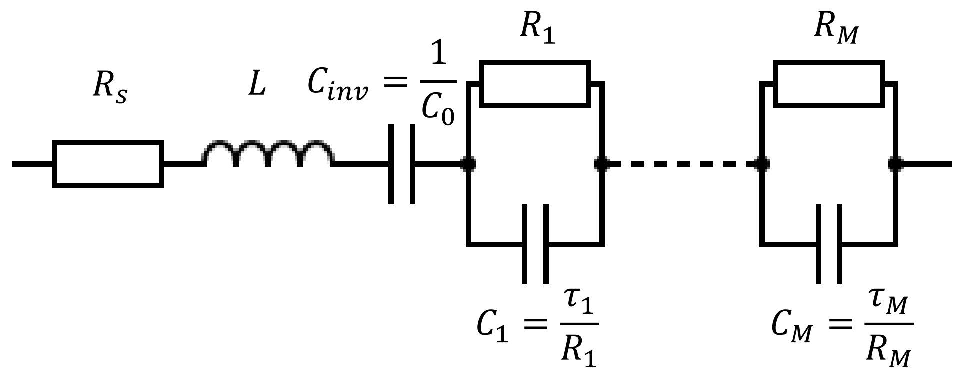

Linear algebra $\boldsymbol{AX} = \boldsymbol{b}$:

$$
\begin{pmatrix}
\sum_{i=1}^{N}\lambda_i & 0 & 0 & \cdots & \sum_{i=1}^{N}\frac{\lambda_i}{1+(\omega_i\tau_M)^2} \\
0 & \sum_{i=1}^{N}\lambda_i\omega_i^2 & -\sum_{i=1}^{N}\lambda_i & \cdots & -\sum_{i=1}^{N}\frac{\lambda_i\omega_i^2\tau_M}{1+(\omega_i\tau_M)^2} \\
\sum_{i=1}^{N}\frac{\lambda_i}{1+(\omega_i\tau_1)^2} & -\sum_{i=1}^{N}\lambda_i & \sum_{i=1}^{N}\frac{\lambda_i}{\omega_i^2} & \cdots & -\sum_{i=1}^{N}\frac{\lambda_i\tau_M}{1+(\omega_i\tau_M)^2} \\
\vdots & \vdots & \vdots & \ddots & \vdots \\
\sum_{i=1}^{N}\frac{\lambda_i}{1+(\omega_i\tau_M)^2} & \sum_{i=1}^{N}\frac{\lambda_i\omega_i\tau_M}{1+\left(\omega_i\tau_M\right)^2} & -\sum_{i=1}^{N}\frac{\lambda_i\tau_M}{\omega_i\left[1+\left(\omega_i\tau_M\right)^2\right]} & \cdots & \sum_{i=1}^{N}\frac{\lambda_i\left[1+\omega_i\tau_M^2\right]}{\omega_i\left[1+\left(\omega_i\tau_M\right)^2\right]^2}
\end{pmatrix}
\begin{pmatrix} R_s \\ L \\ C_{inv} \\ \vdots \\ R_M \end{pmatrix}
=
\begin{pmatrix}
\sum_{i=1}^{N}\lambda_i Re_i \\
\sum_{i=1}^{N}\lambda_i\omega_i Im_i \\
\sum_{i=1}^{N}\frac{\lambda_i}{\omega_i}Im_i \\
\vdots \\
\sum_{i=1}^{N}\frac{\lambda_i(Re_i-\omega_i\tau_M Im_i)}{1+(\omega_i\tau_M)^2}
\end{pmatrix}
$$

Singular value decomposition (SVD) to solve $\boldsymbol{X}$.

Schönleber, M., Klotz, D. and Ivers-Tiffée, E., 2014. A method for improving the robustness of linear Kramers-Kronig validity tests. Electrochimica Acta, 131, pp.20-27.
Boukamp, B.A., 1995. A linear Kronig-Kramers transform test for immittance data validation. Journal of the electrochemical society, 142(6), p.1885.

II) Practical aspects, analyses, and applications

Smooth, LC correction, extrapolation based on KK test

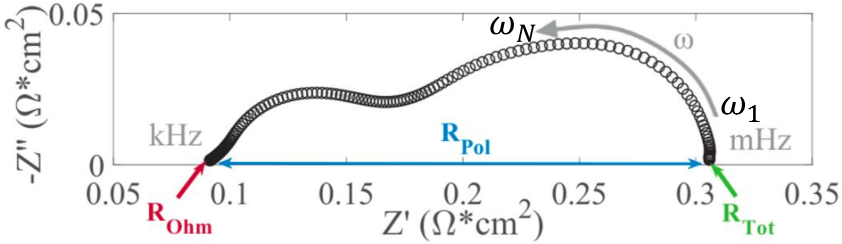

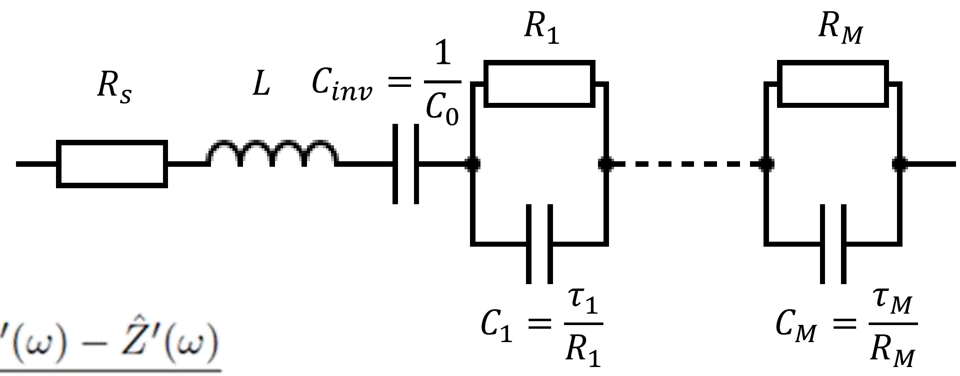

$$\Delta_{Re} = \frac{Z'(\omega) - \hat{Z}'(\omega)}{|Z(\omega)|}$$

$$\Delta_{Im} = \frac{Z''(\omega) - \hat{Z}''(\omega)}{|Z(\omega)|}$$

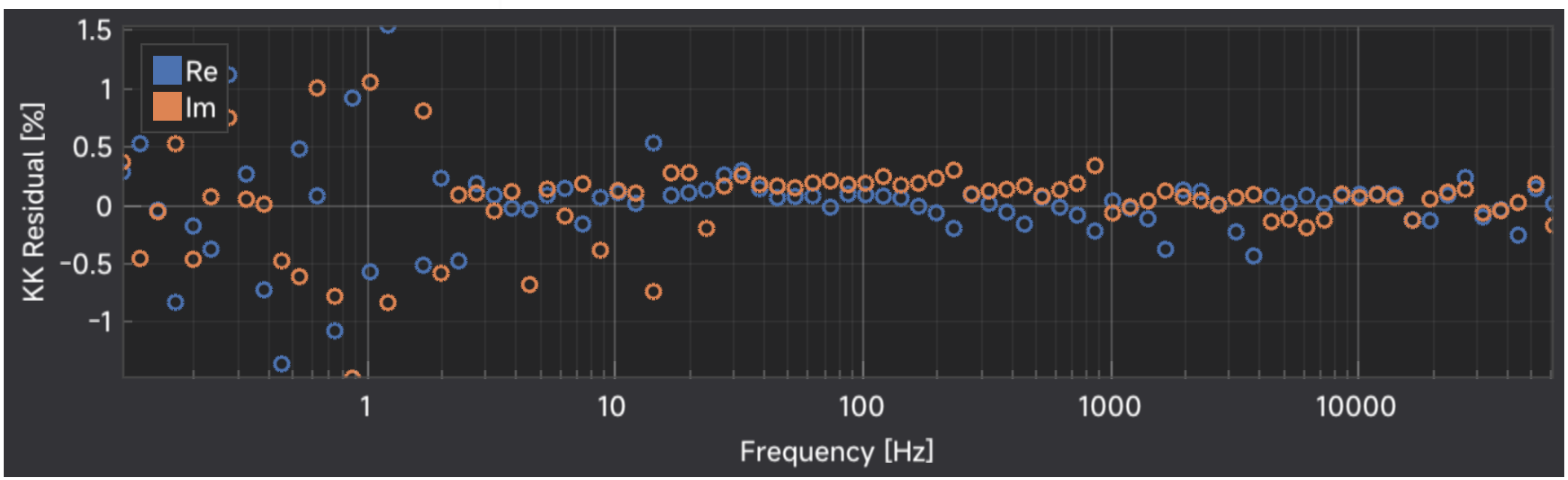

II) Practical aspects, analyses, and applications

Smooth, LC correction, extrapolation based on KK test

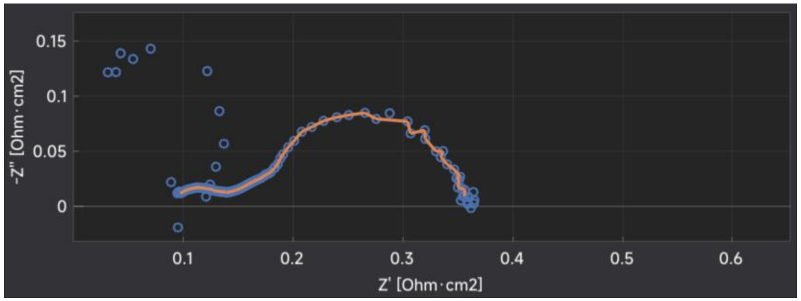

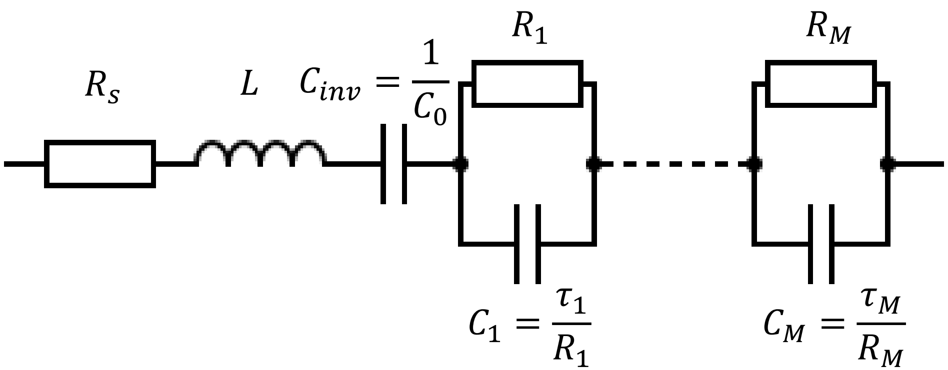

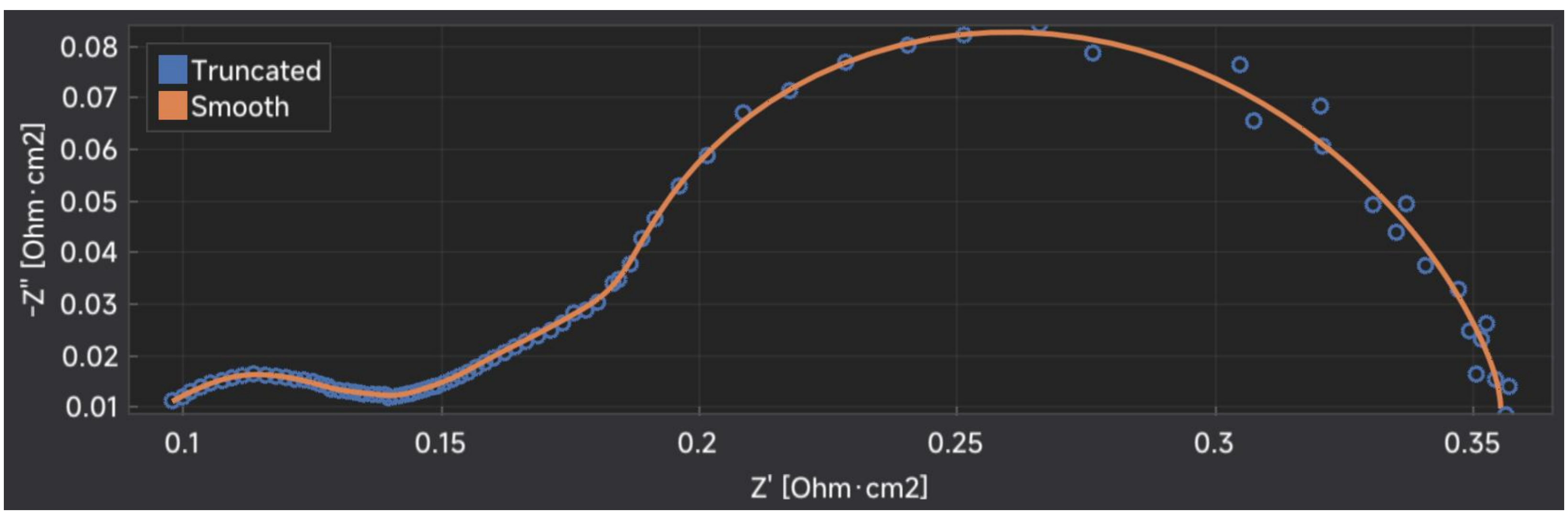

II) Practical aspects, analyses, and applications

Smooth, LC correction, extrapolation based on KK test

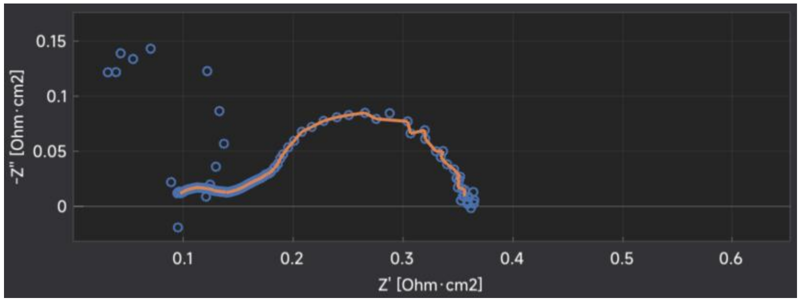

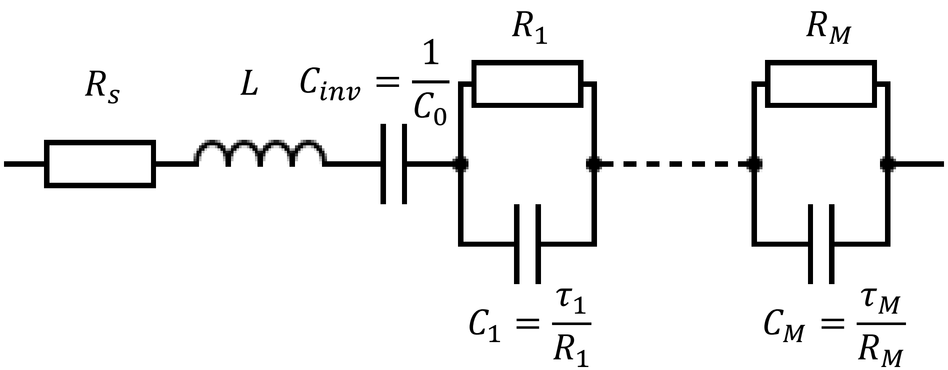

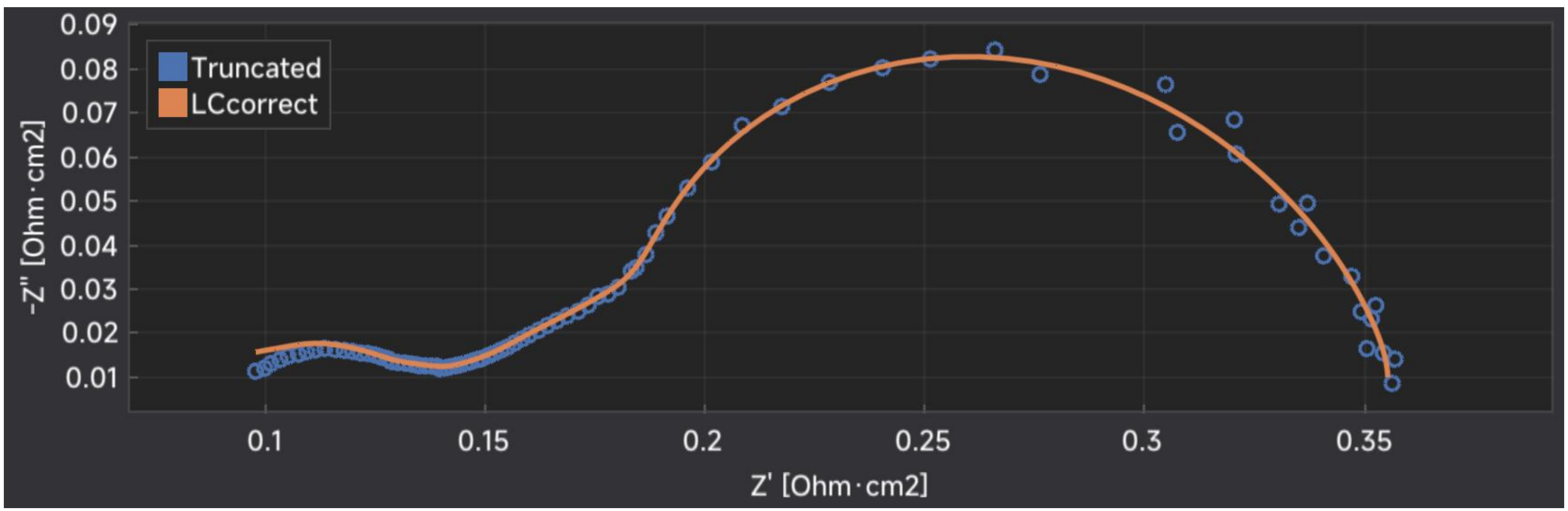

II) Practical aspects, analyses, and applications

Smooth, LC correction, extrapolation based on KK test

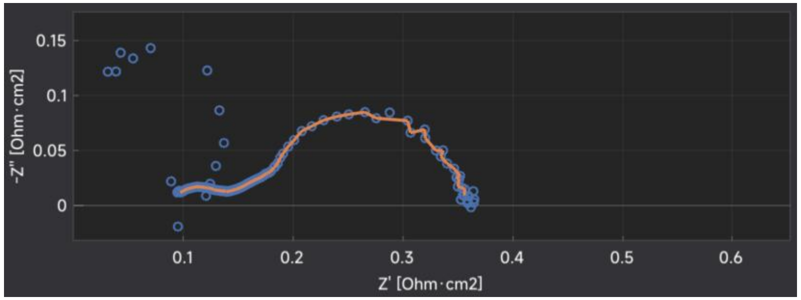

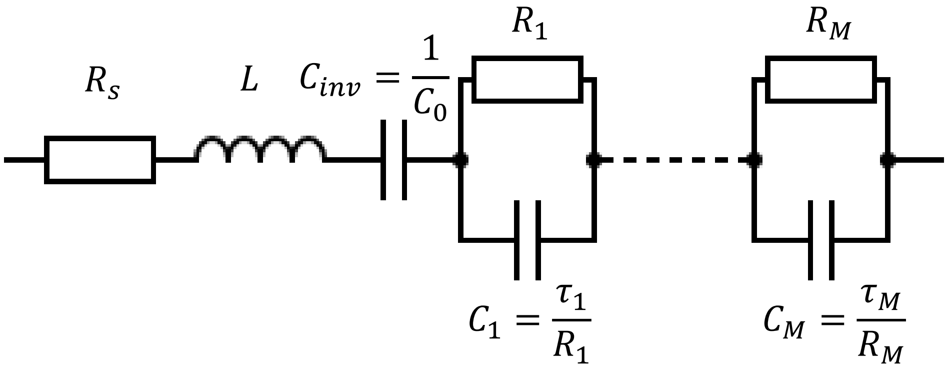

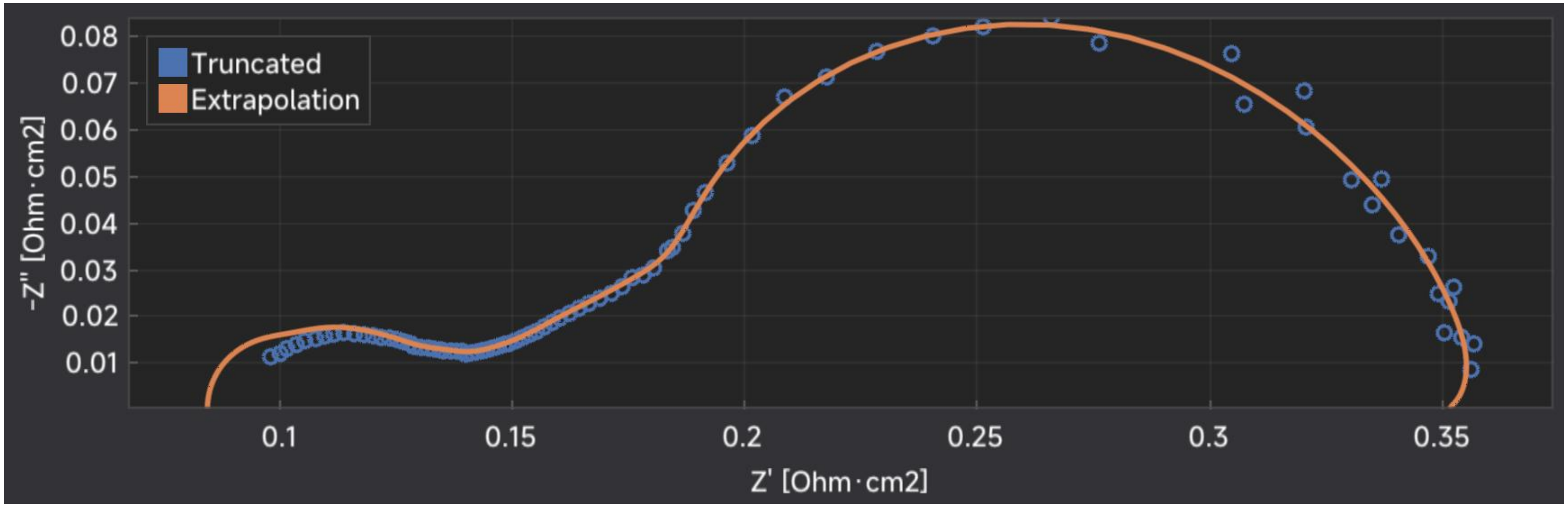

II) Practical aspects, analyses, and applications

Distribution of Relaxation Times (DRT)

$$Z(\omega) = R_{ohm} + \sum_{i=1}^{N} \frac{R_i}{1 + j\omega\tau_i}$$

$$\tau_i = R_i C_i$$

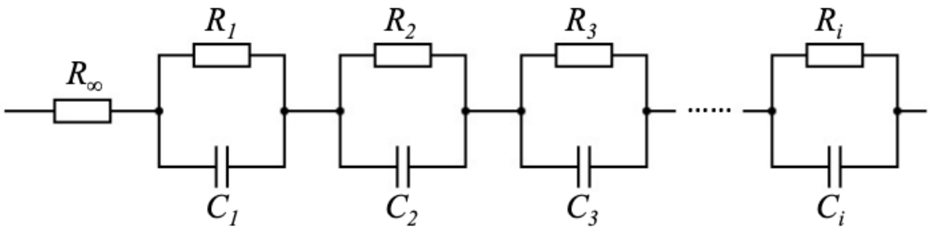

Generalized Voigt model

Discrete function

Continuous function

$$Z(\omega) = R_{ohm} + \int_0^{\infty} \frac{R(\tau)}{1 + j\omega\tau}\, d\tau$$

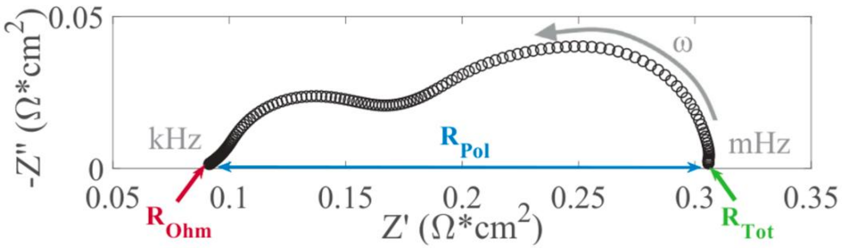

$$Z(\omega) = R_{ohm} + R_{pol} \int_0^{\infty} \frac{\gamma(\tau)}{1 + j\omega\tau}\, d\tau$$

$$R(\tau) = R_{pol} \cdot \gamma(\tau)$$

$$\int_0^{\infty} \gamma(\tau)\, d\tau = 1$$

II) Practical aspects, analyses, and applications

Distribution of Relaxation Times (DRT)

$$Z(\omega) = R_{ohm} + R_{pol}\int_0^{\infty}\frac{\gamma(\tau)}{1+j\omega\tau}\,d\tau$$

$$R(\tau) = R_{pol}\cdot\gamma(\tau)$$

$$\int_0^{\infty}\gamma(\tau)\,d\tau = 1$$

$$Z(\omega) - R_{ohm} = R_{pol}\int_0^{\infty}\frac{\gamma(\tau)}{1+j\omega\tau}\,d\tau$$

$$Z(\omega) = Z'(\omega) + jZ''(\omega)$$

$$Z'(\omega) - R_{ohm} = R_{pol}\int_0^{\infty}\frac{\gamma(\tau)}{1+(\omega\tau)^2}\,d\tau$$

$$Z''(\omega) = R_{pol}\int_0^{\infty}\frac{\omega\tau\cdot\gamma(\tau)}{1+(\omega\tau)^2}\,d\tau$$

Inverse ill-posed problem

- **A solution exists;**
- **The solution is unique**
- **The solution's behavior changes continuously with the initial conditions**

$$\boldsymbol{Z} = \boldsymbol{A\gamma} \qquad A = \frac{1}{1+j\omega\tau}$$

$$\boldsymbol{\gamma} = arg\min_{\boldsymbol{\gamma}}(\|\boldsymbol{Z}-\boldsymbol{A\gamma}\|^2) \Rightarrow \boldsymbol{\gamma} = (\boldsymbol{A^TA})^{-1}\boldsymbol{A^TZ}$$

Tikhonov regularization (λ as regularization factor**)**

$$\boldsymbol{\gamma} = arg\min_{\boldsymbol{\gamma}}(\|\boldsymbol{A\gamma}-\boldsymbol{Z}\|^2 + \lambda\|\boldsymbol{L\gamma}\|^2)$$

$$\mathbf{L} = \begin{bmatrix} 1 & 1 & 1 & 1 & \cdots \\ 1 & 1 & 1 & 1 & \cdots \\ \vdots & \ddots & \ddots & \ddots & \ddots \end{bmatrix}$$

$$\Rightarrow \boldsymbol{\gamma} = (\boldsymbol{A^TA} + \lambda\boldsymbol{L^TL})^{-1}\boldsymbol{A^TZ} \Rightarrow$$

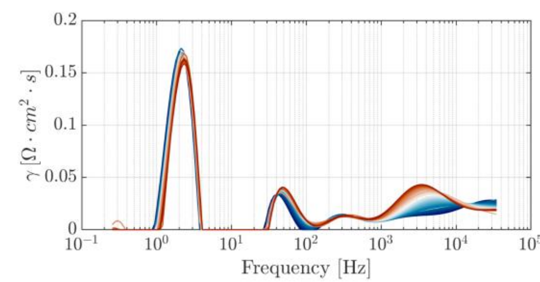

II) Practical aspects, analyses, and applications

DRT for Solid Oxide Cells (650-850 °C)

Cell type 1

	RQ7 Gas conversion	RQ6 O^{2-} surface exchange in GDC	RQ5 Negatrode and positrode gas diffusion	RQ4 Positrode charge transfer	RQ3 Negatrode charge transfer
Parameters - statistic	$i > FU > p_{H_2O}$	$T > p_{H_2O}$	$T > p_{H_2} > p_{H_2O}$	$T > AU$	$i > FU > T$
Temperature ↑	↖	↙	↙	↓	↙↘
Current density ↑ at fixed FU/AU	↘	↘	↘	↘	↘
Current density ↑ at fixed gas flow	↘	↖	↗	-	-
H_2 partial pressure ↑	↓	→	-	-	↙
H_2O partial pressure (SH) ↑	↘↙	↗	↘	→←	↑
O_2 partial pressure ↑	-	↘	↘	↘	→
Frequency	0.1-1 Hz	0.1-10 Hz	1-50 Hz (Partially overlapped with O^{2-} surface exchange)	50-150 Hz	> 150 Hz

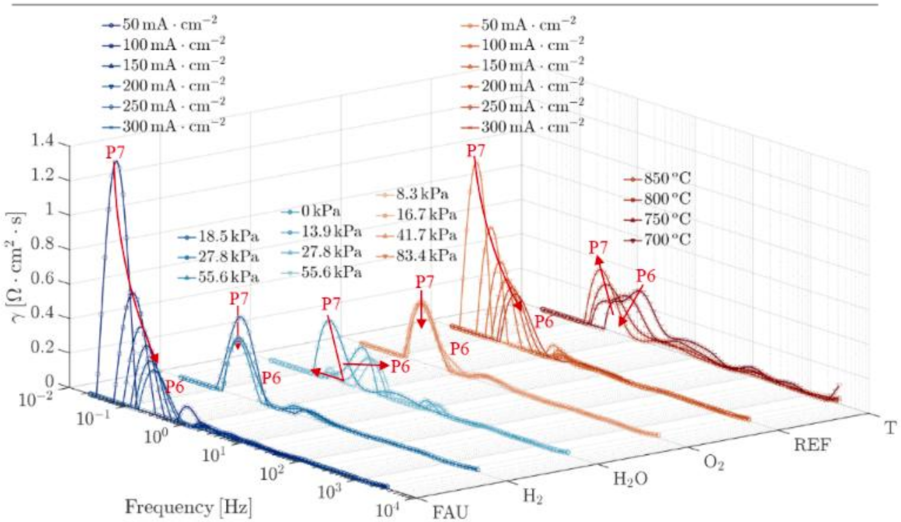

Cell type 2

	P1 Conversion diffusion at low pO_2 transport in reforming mixture	P2 Gas conversion	P3 Fuel electrode diffusion/ oxygen electrode reaction + solid state diffusion	P4 Secondary peaks (fuel and oxygen electrode transport)	P5 Fuel electrode charge transfer	P6 High f. peak (?)
Parameters	$pO_2 > P$	$F_{tot} > pH_2O > P > i$	$pH_2O > i > pO_2 > P$	$pH_2O > T > P$	$T > i > pH_2O > P$	T
Temperature (T) ↑	-	-	-	↓	↘	↓
Current density (i) ↑	-	↺	↙	↓	↘	-
Oxygen partial pressure (pO_2)↑	↘	-	↓	-	-	-
Steam partial pressure (pH_2O)↑	-	↓	↓	↘	↘	-
Total flow rate (F_{tot})↑	-	↘	-	-	-	-
Pressure (P)↑	⟵	↙	↙	↓	↓	-
Frequency	< 1Hz	1-10 Hz	10-100 Hz	0.1-0.5 kHz	0.5-up to 100 kHz *	5- up to 200 kHz *
Single cell no L	0.1	4	50	0.5	20 (2)	200 (6)
Segmented SRU	0.3	4	40	0.3	1	5
Short Stack	0.2	1	20	0.1	0.4	2

* Characteristic frequency influenced by inductance and frequency range

() values obtained in a different experiment with respect to the sensitivity one

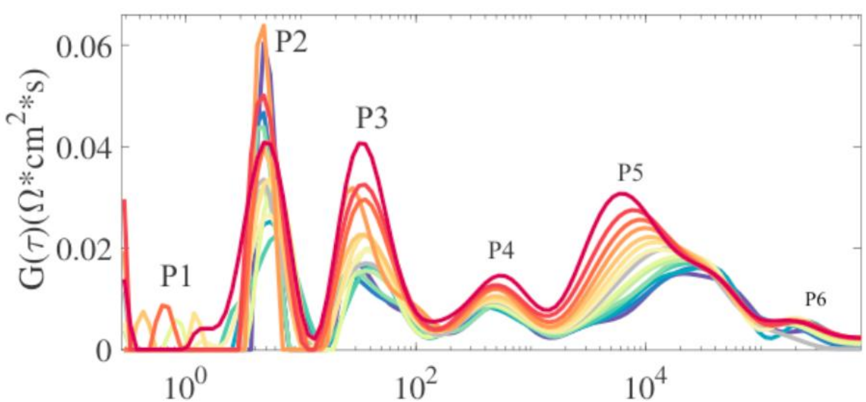

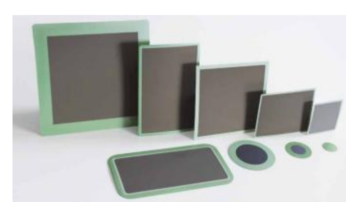

II) Practical aspects, analyses, and applications

DRT for Proton Conducting Cells (400-600 °C)

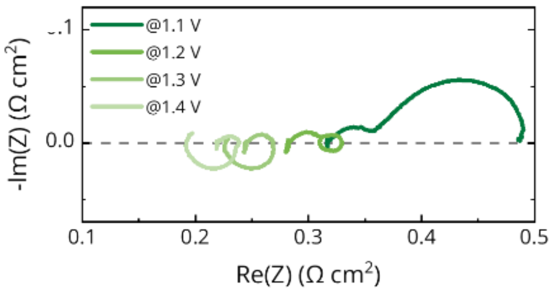

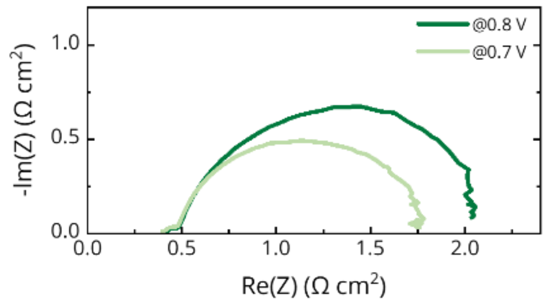

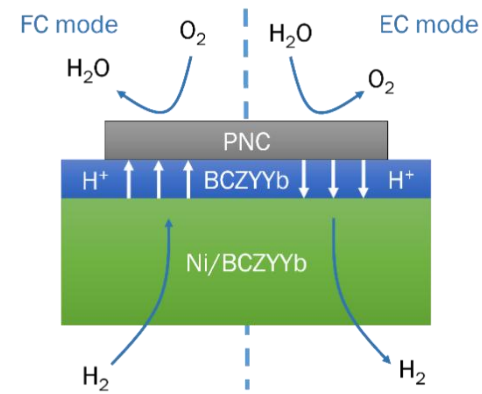

Active area: 12.56 cm^2

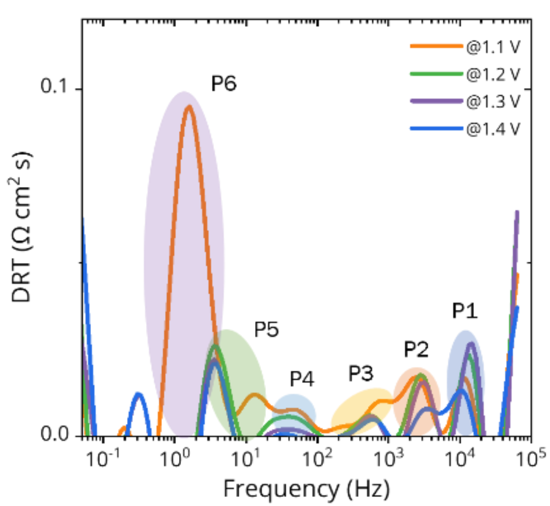

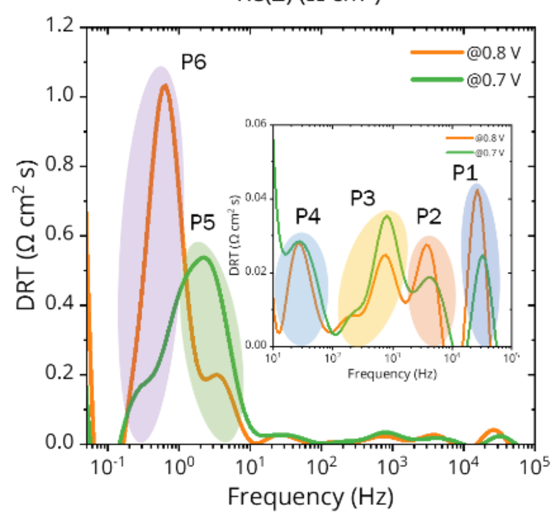

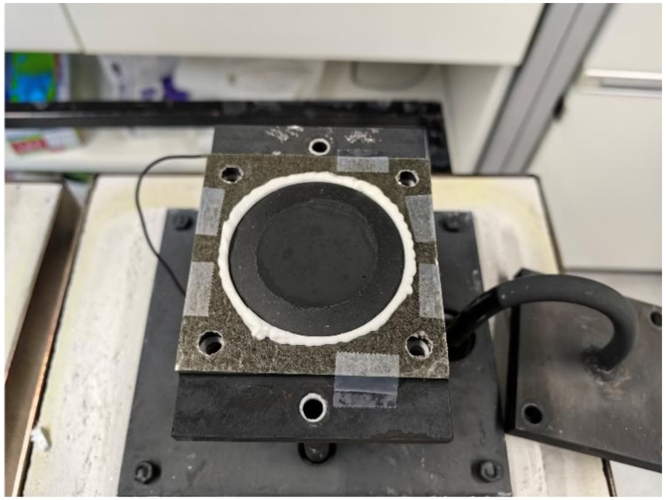

II) Practical aspects, analyses, and applications

DRT for Proton exchange membrane cells (<100 ºC)

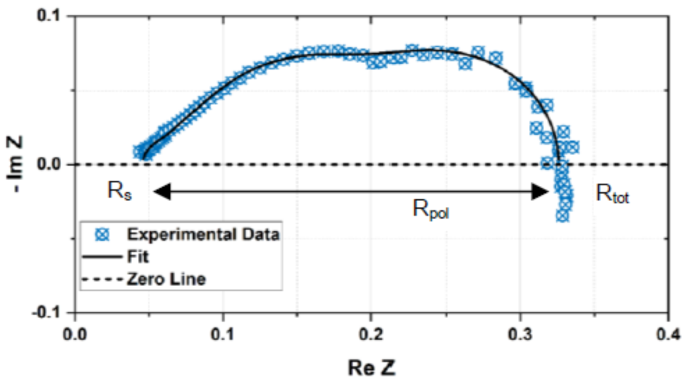

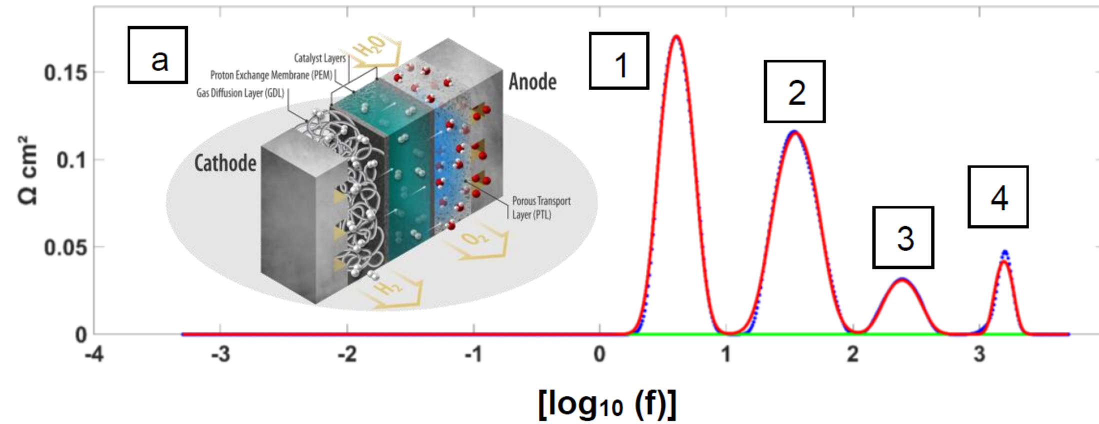

Table 1: The DRT peak positions and the corresponding area in Ω cm². The peak ASR values are color coded from red (highest) to green (lowest).

Process Number [-]	Peak Position [$\log_{10}$ (f)]	Peak Position [Hz]	Peak Area [Ω cm²]	Literature process assignment	Refs.
1	0.6069	4.0585	0.1282	unknown	
2	1.5484	34.1661	0.1142	Gas diffusion	
3	2.3875	242.1380	0.0243	ORR	[7–10]
4	3.1929	1574. 5163	0.0166	H^+ transfer	

II) Practical aspects, analyses, and applications

DRT for Anion Exchange Membrane Cells (<100 °C)

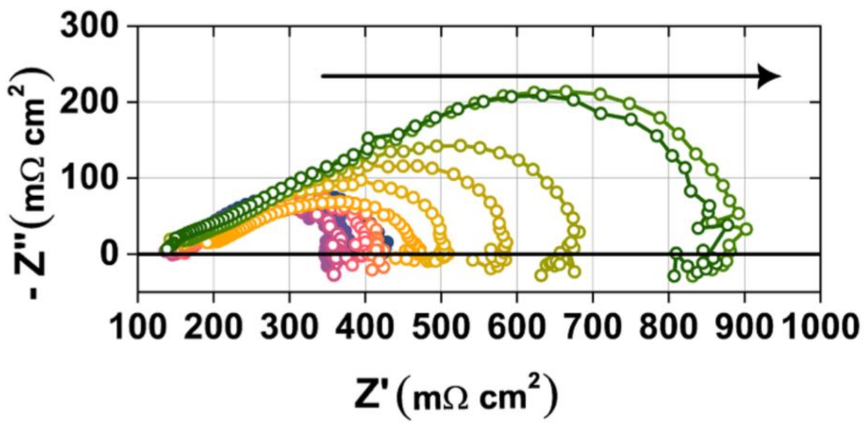

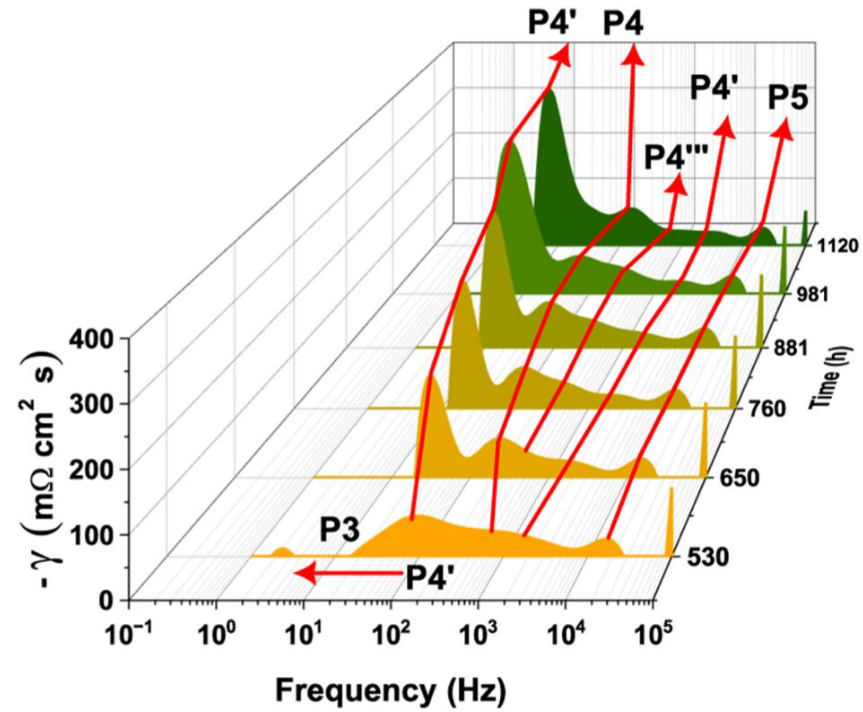

MEA peaks	H_2 half-cell peaks	O_2 half-cell peaks	frequency range (Hz)	process description	refs
P1			1−5	water and gas diffusion-related process of HER, OER electrodes	this work extending[24]
P2			5−20		
P3			25−80		
P4	P4(i) H_2	P4(i) O_2, P4(ii) O_2	60−2000	HER, OER charge transfer	24
P5		P5O_2	2200−3200	OER ion transport	this work extending[24]
P5	P5H_2		7000−9000	HER ion transport	this work extending[24]

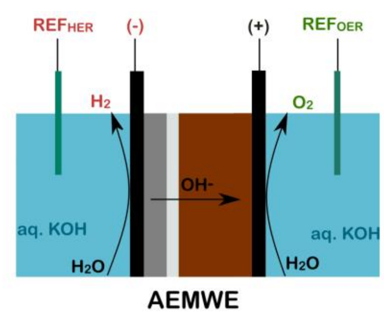

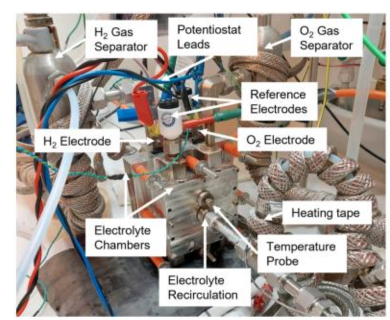

II) Practical aspects, analyses, and applications

2) Data treatment

Complex Nonlinear Least Square fitting (CNLS)

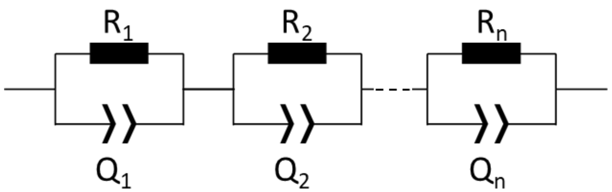

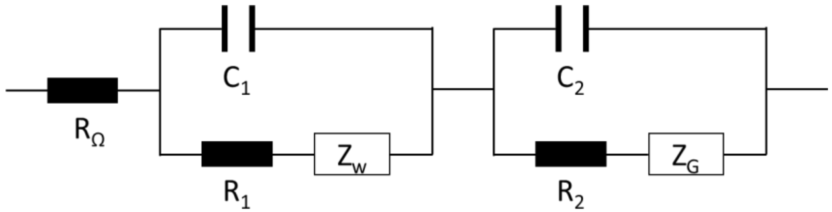

Minimization of the sum of squares function:

$$S = \sum_{i=1}^{N} w_i \left(\left[Z'_i(\omega_i) - Z'_{M,i}(\omega_i, x) \right]^2 + \left[Z''_i(\omega_i) - Z''_{M,i}(\omega_i, x) \right]^2 \right)$$

where $Z_i(\omega)$ and $Z_{M,i}(\omega,x)$ are the measured and modeled impedance, respectively and w_i is the weight factor $w_i = \left[Z_{Re,i}{}^2 + Z_{Im,i}{}^2 \right]^{-1}$

element	impedance	process
(R) serial resistor	R	contact and electrolyte resistance
(RQ) resistor and a constant phase element in parallel	$\frac{R}{1+RQ_0(j\omega)^n}$	double layer capacitance and charge-transfer reactions in parallel
(G) Gerischer element	$\frac{R_{\text{chem}}}{\sqrt{1+j\omega t_{\text{chem}}}}$	combination of electrochemical charge-transfer and diffusion
(W) Warburg element	$R_{\text{w}}\frac{\tanh[(j\omega T)^\alpha]}{(j\omega T)^\alpha}$	diffusion processes
(TLM) transition line model	$\frac{R_{\text{el}}R_{\text{ion,L}}}{R_{\text{el}}+R_{\text{ion,L}}}\left(L+\frac{2\lambda}{\sinh(L/\lambda)}\right)+$ $\lambda_{TLM}\frac{R_{\text{el}}^2+R_{\text{ion,L}}^2}{R_{\text{el}}+R_{\text{ion,L}}}\coth\left(\frac{L}{\lambda_{\text{TLM}}}\right)$	porous electrode electrochemistry

II) Practical aspects, analyses, and applications

3) Non linear systems: Total Harmonic Distorsion

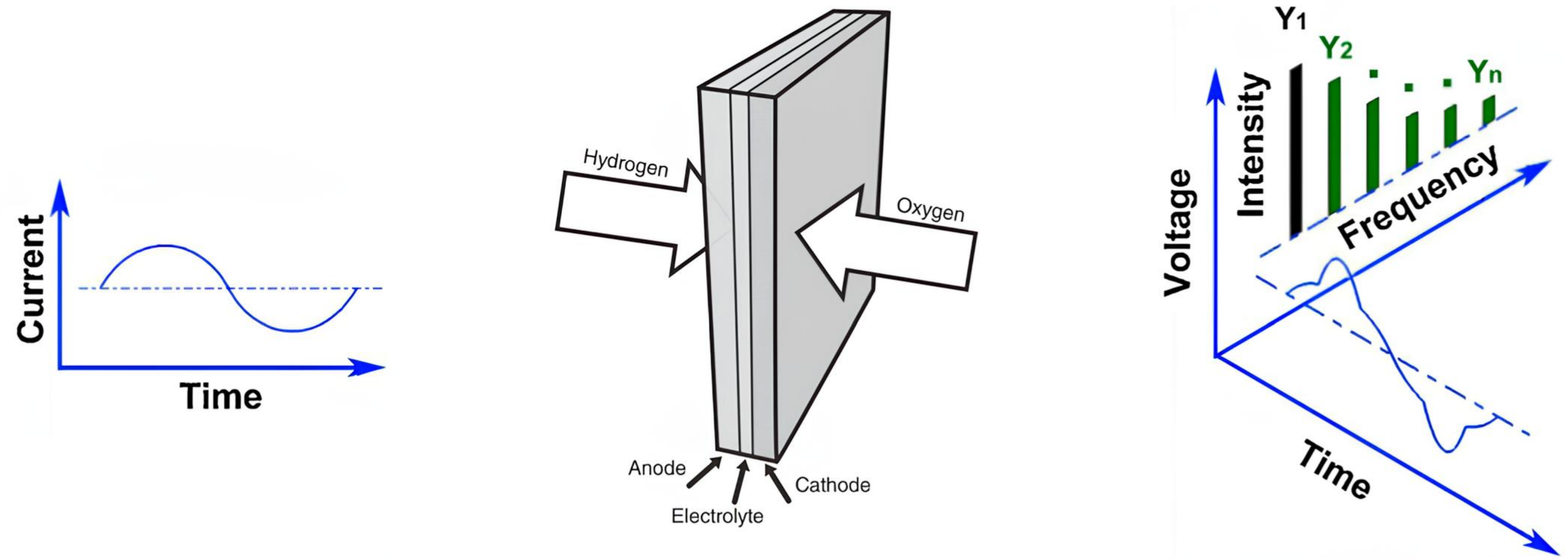

Input current signal → **Fuel cell** → **Output voltage response**

$$\mathrm{THD} = \frac{\sqrt{\sum_{n=2}^{\infty} Y_n^2}}{Y_1}$$